Threshold Charged Photopion Production

A Letter-of-Intent to the MAX-lab PAC
Submitted 2 May, 2002

Kevin Fissum
Lund University
SE-221 00 Lund
Sweden
kevin.fissum@nuclear.lu.se

Grant O'Rielly
The George Washington University
Washington, DC 20052
USA
orielly@gwu.edu

Abstract

In this letter-of-intent, we present a series of five charged pion photoproduction experiments, all at-or-near reaction threshold. Each experiment builds on the experience gained and results obtained in the previous one, in our relentless drive towards threshold. With our passive target measurements, we will better the best world data for π^+ photoproduction by a factor of two in terms of photon energy resolution. With our active target measurements, our goal is to produce high quality data as close to threshold as possible, and subsequently complement these measurements with a groundbreaking threshold π^- photoproduction measurement. From these data, we will extract precision results for the threshold E_{0+} (s-wave) amplitudes for charged pion photoproduction as a test of QCD-based theoretical predictions.

Contents

1 Introduction

Pion photoproduction from the nucleon is a fundamental process which has enjoyed renewed interest, both theoretically and experimentally, in the past several years. Experimentally, the availability of CW electron accelerators and quasi-monochromatic photon beams produced using techniques such as laser back-scattering and bremsstrahlung photon tagging have provided the opportunity for high-quality measurements with small statistical uncertainties and well-understood systematic uncertainties, compared with the potentially large uncertainties of earlier measurements performed with bremsstrahlung photon beams. These experiments are being performed at laboratories such as SPring-8 in Osaka, Japan, Jefferson Lab in the United States, and GRAAL in Grenoble, France, at photon energies well above the pion production threshold, in order to study baryon properties and to identify and investigate resonances in the hardonic systems. At lower energies, facilities such as LEGS at Brookhaven in the United States, MAMI at Mainz, Germany, the Saskatchewan Accelerator Lab in Canada, and the new accelerator and photon tagging facility being developed at MAX-lab in Lund, provide the opportunity for precision measurements of pion photoproduction near threshold. Together, these new facilities afford the opportunity to obtain high-quality data that can be compared with the predictions of modern QCD-based theories, and which are essential to the performance of Partial-Wave Analyses (PWA) studies based on the world's database of pion electro- and photoproduction data.

Near threshold, measurements of pion photoproduction from the nucleon are one of the few low-energy phenomena for which QCD-based theories can be formulated and tested. As such, measurements of these reactions form an important check on our understanding of the underlying dynamics in the nucleon system. The four reaction channels for pion photoproduction from the nucleon are:

$$\gamma + p \longrightarrow n + \pi^+$$

$$\gamma + n \longrightarrow p + \pi^-$$

$$\gamma + p \longrightarrow p + \pi^\circ$$

$$\gamma + n \longrightarrow n + \pi^\circ$$

At energies close to threshold, the relative angular momentum between the nucleon and pion is predominately s-wave ($l = 0$), with some small p-wave ($l = 1$) component. Since the p-wave component is proportional to the pion momentum in the center-of-mass frame, this contribution goes to zero at threshold,

while the s-wave contribution remains finite.

$$\sigma_{\text{total}} = 4\pi \left(\frac{q}{k}\right) \left\{ |\mathrm{E}_{0^+}|^2 + |\text{p-wave}|^2 \right\},$$

where σ_{total} is the total measured cross section, q is the pion momentum, and k is the photon momentum. Thus, measurements of the pion photoproduction cross section close to threshold allow for a direct measurement of the s-wave amplitudes, and enable the extraction of the fundamental amplitude E_{0^+}.

The leading order terms of the E_{0^+} amplitude have been predicted in a model-independent manner using Low-Energy Theorems (LET) based on current algebra and partially-conserved axial current (PCAC). More recently, Chiral Perturbation Theory (ChPT), which is a method for solving QCD at low energies, has been applied to this process. ChPT calculations include higher-order terms in the evaluation of the E_{0^+} amplitude predictions. The predictions from both ChPT and earlier Low-Energy Theorems for pion photoproduction from the nucleon are listed below:

Channel	ChPT ($\times 10^{-3} m_\pi^{-1}$)	LET ($\times 10^{-3} m_\pi^{-1}$)	recent expt. value ($\times 10^{-3} m_\pi^{-1}$)
$\gamma + p \to n + \pi^+$	$+28.2 \pm 0.6$	$+27.6 \pm 0.2$	$+28.2 \pm 0.6$
$\gamma + n \to p + \pi^-$	-32.7 ± 0.6	-31.7 ± 0.2	-31.5 ± 0.8
$\gamma + p \to p + \pi^\circ$	-1.16	-2.3	-1.32 ± 0.08
$\gamma + n \to n + \pi^\circ$	$+2.6$	-0.5	~ -0.4

Much of the recent experimental effort has gone into studying π° photoproduction since the predictions based on the newer ChPT techniques are quite different from the older predictions based on the LETs. For the charged π channels, the existing data is mostly over 20 years old, with only two modern measurements having been performed - one each on the π^+ and π^- channels.

In addition to extracting values of the amplitudes for comparison with theoretical predictions, pion production near threshold permits the issue of isospin symmetry in the electromagnetic interaction to be addressed. Ultimately, violation of isospin symmetry is related to the light quark mass difference, $m_u - m_d$, together with virtual photon effects. Since systems involving nucleons can exhibt these effects at leading order, pion photoproduction is well suited for such investigations. Due to the triangle relation that exists between one of the physical amplitudes and the three others [1], accurate measurements of the E_{0^+} amplitudes in all four pion photoproduction channels would enable this question to be addressed. These isospin symmetry violation effects are masked to a large extent since the quark mass difference is small compared

to the scale of the strong interaction ($\approx$1 GeV). Thus, to access the effect of the quark mass difference on isospin symmetry violation, accurate calculations and precise measurements are required.

In the specific case of charged pion photoproduction, due to the leading Born terms, the contribution of the pion-loop diagrams is small, and the chiral expansion is rapidly converging, leading to reliable theoretical predictions from ChPT. Consequently, investigation of the charged pion photoproduction channels can provide information and constraints on the πN scattering lengths and the πN coupling constant $g_{\pi \mathrm{N}}$. Accurate measurements of the charged pion photoproduction channels also allows for the investigation of isospin symmetry, when combined with accurate determination of the neutral pion photoproduction channels.

Experimentally, the most recent measurement of the $\gamma + p \to n + \pi^+$ reaction has been performed at SAL [2], an experiment which measured the cross section to within 1 MeV of threshold, and extracted a value for $\mathrm{E}_{0^+}^{(\pi^+ n)}$ consistent with the prediction of ChPT. The most recent value for $\mathrm{E}_{0^+}^{(\pi^- p)}$ has been extracted from a measurement of the inverse capture reaction $\pi^- + p \to \gamma + n$ [3]. There has been, to our knowledge, no recent direct measurement of the $\gamma + n \to p + \pi^-$ reaction.

The overall agreement between these measurements and the theoretical predications is reasonably good, however the ChPT predictions are somewhat larger than the most recent data for both charged pion channels. We note that in particular, for the $\gamma + p \to n + \pi^+$ reaction, the extracted value for $\mathrm{E}_{0^+}^{(\pi^+ n)}$ depended on the details of the extrapolation to threshold. The final value ranged from $(27.82 \pm 0.27) \times 10^{-3} m_\pi^{-1}$ (assuming E_{0^+} to be constant), to $(28.29 \pm 0.70) \times 10^{-3} m_\pi^{-1}$ (based on a two-parameter linear fit). The variation in the E_{0^+} value is comparable with the quoted uncertainties in the measurement; however, it would be useful to further reduce the uncertainty in this extrapolation. Additional measurements will complement the existing data and improve our understanding of this energy dependence, which is related to the p-wave contribution to the cross section.

2 The proposed experiment program

The experiment program detailed in the remainder of this letter-of-intent is presented in Table 1. We propose a series of five experiments.

Name	E_γ (MeV)	ΔE_γ (keV)	δ_{stat} (%)	detected particle	beam time (hr)	real time (week)
Near threshold $H(\gamma,\pi^+)$	161.5 - 171.0	340	3.0	π^+	325	3
π^+ photoproduction via coincident detection of the π^+ and neutron	161.5 - 164.0	(340)	(2.0)	(π^+)		
very close to threshold	153.0 - 164.0	340	1.0	neutron	450	3
High-luminosity measurements of threshold π^+ photoproduction	(150.0) - 161.0	170	3.0	neutron	125	3
Threshold Photoproduction of π^+	(150.0) - 161.0	170	2.0	π^+	335	3
Near-threshold Photoproduction of π^-	(150.0) - 161.0	340	4.0	π^-,γ'	325	3

Table 1
An overview of the proposed series of experiments.

The program begins with three passive target measurements, and ends with two active target measurements. The experiments are rather straightforward at the beginning of the program, but the complexity ramps up rapidly. The evolution of measurements allows us to fully understand the performance of the accelerator and tagging system together with our detector systems. Each successive measurement builds on the experience we obtain in the previous measurement(s), thus ensuring our understanding of the behavior of the entire system and giving us confidence that the subsequent measurement can be achieved to the desired level of statistical and systematic uncertainties. Thus, each measurement is essential - no one can be skipped over, and no two can be combined.

2.1.1 Overview

In this first experiment in the anticipated program, we shall measure absolute cross sections for $\gamma + p \longrightarrow n + \pi^+$ as close to the reaction threshold ($E_\gamma = 151.44$ MeV) as possible using the newly commissioned high-resolution tagged photon facility at MAX-lab. Pions will be detected in well-understood fast plastic ΔE-E scintillator telescopes[1] with moderate energy resolution optimized to identify π^+s via their decay to a μ^+. We will employ thin, solid targets to minimize π^+ energy loss and simplify the overall normalization. Particle identification will be performed both at the hardware and software levels via well-established techniques. Our goal is to reproduce world results with a photon energy resolution of 340 keV and a 3% statistical error over the energy regime 9-20 MeV above threshold. This measurement will then serve as an ongoing normalization measurement for the second experiment (see Section 2.2) in the program.

Because of its self-calibrating and self-normalizing nature, we feel this experiment is an excellent candidate with which to initiate the π^+ photoproduction program at the upgraded MAX-lab tagged photon facility.

2.1.2 Measurement details

Fig. 1 shows an overview of the experiment hall.

Photon beam

We anticipate a 10 nA, 200 MeV continuous electron beam, which we will use to produce a CW tagged-photon beam via a thin, low-Z radiator (100 μm Al). The continuity of the beam will be continuously monitored [4]. We will employ the (former) SAL end-point tagger (ET) [5] and the Lund focal-plane array (64 counters) [6]. The above combination should yield a recoil electron rate per tagger counter of 1 MHz. We anticipate collimating the photon beam to 12 mm in diameter. We will make multiple, dedicated low-intensity tagging efficiency measurements as experimentally convenient to set the absolute scale of the photon flux. We anticipate a tagging efficiency of 40%. We will monitor the relative tagging efficiency continuously using a dedicated standalone beam monitor [7]. We anticipate that π^+s with $T_{\pi^+} < 15$ MeV will be energetically forbidden from reaching the detectors. We will thus tag an 11 MeV photon-

[1] (at least one) telescope to be provided by Bo Jakobsson, Professor of Cosmic and Subatomic Physics, LU.

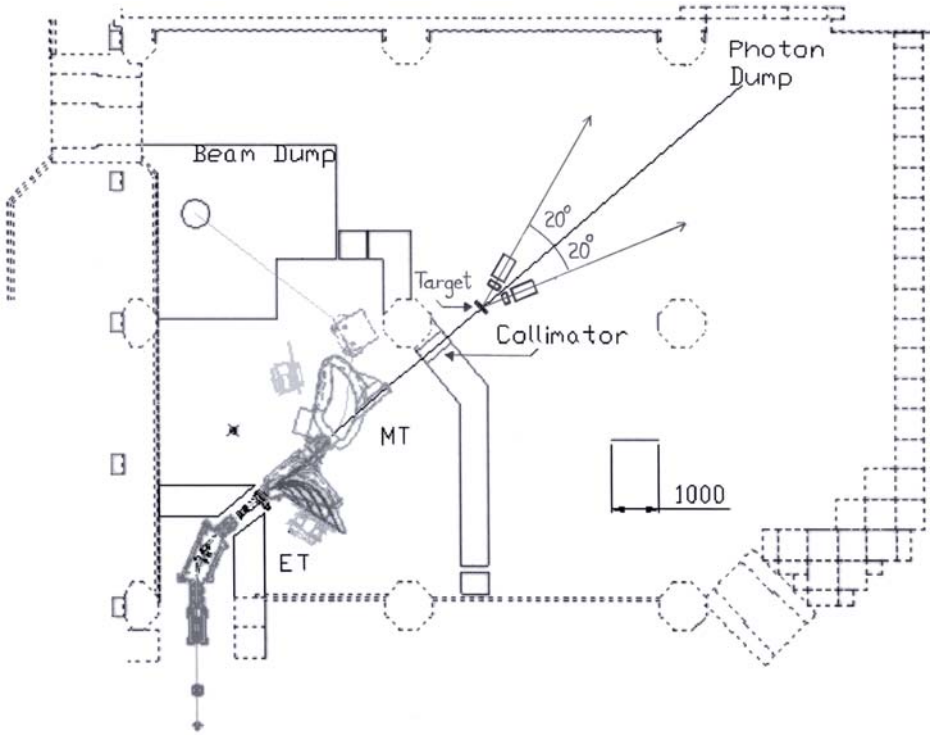

Fig. 1. The proposed configuration of the experiment hall for this experiment.

energy bite from 160 MeV $< E_\gamma <$ 171 MeV (corresponding to π^+s from 13.5 MeV $< T_{\pi^+} <$ 25.5 MeV at $\theta_{\pi^+} = 20°$), with a per-counter resolution on the order of 170 keV [8]. Roughly 10% of the spectrometer acceptance (six tagger counters) will be used to tag in an energetically forbidden region - data which are very useful for eventual background subtractions.

Targets and detectors (X-arm)

For this measurement, we will use thin, solid, isotopically understood CH_2 and C targets which are commercially available. The CH_2 target will be 300 mg/cm^2, and the areal density of C scattering centers in both targets shall be roughly the same (on the order of 240 mg/cm^2). The targets will be mounted in a remote-controlled target ladder together with an empty slot for measurements of room background. The targets will be placed approximately 1 m downstream of the photon beam collimator.

We anticipate using at least one ΔE-E plastic scintillator telescope (such as those reported in [9,10]) as a π^+ detector. A hardware coincidence between the recoil electron in the tagger focal plane and the X-arm will be made. An additional telescope would be placed at the same angle ($\theta_{\pi^+} = 20°$) on the opposite side of the photon beam to measure the same cross section (and thus test our systematics). The telescope(s) will be shielded extensively with Pb, collimated to 5 cm in diameter, and placed as close to the target as reasonable (25 cm) to keep the loss of π^+ to decay-in-flight ($\overline{\tau} = 26$ ns) to below 5%.

Quantity	Description
E_{beam}	200 MeV
I_{beam}	10 nA
radiator	100 μm Al
tagger	SAL end-point (ET)
focal-plane array	Lund 64-counter (6 counters below π^+ threshold)
E_γ bite	160 MeV $< E_\gamma <$ 171 MeV (11 MeV)
ΔE_γ	170 keV
$\dot{N}_e$ per counter	1 MHz
collimator	12 mm diameter
absolute $\varepsilon_{\rm tagg}$ measurements	multiple
relative $\varepsilon_{\rm tagg}$ measurements	yes
$\varepsilon_{\rm tagg}$	40%

Table 2
A summary of the anticipated beam parameters. These parameters have been established based on experience gained at SAL [5] and MAX-lab [6].

Target	Thickness (mg/cm^2)
CH_2	300
C	255
blank	N/A

Table 3
A summary of the anticipated target parameters. The thickness of CH_2 is chosen as a trade-off between event rate and π^+ energyloss in the target. The thickness of C is chosen to match the C-content of the CH_2 target.

We thus anticipate a solid angle of 125 msr. Energy resolution is not an issue. Fundamentally, the detector relies on identifying 4.12 MeV μ^+ afterpulses associated with the decay of the π^+ as a means of particle identification complementary to standard ΔE-E techniques. We intend to look for these decay pulses over the 100 ns subsequent to the primary π^+ event. High-quality delay lines with low dispersion and low loss (RG-8 or better) will be used to optimize the quality of the decay pulses. The advantage of this technique is that the absolute detection efficiency may be readily calculated (we anticipate 10%). We will accept pileup on the level of 0.5%, so that a 50 kHz singles rate in the telescopes will constrain the maximum beam current. Efficiency loss due to π^+N interactions in the scintillator plastic will be addressed with simulation. A more complete description of the experimental circuit is presented in

Quantity	Specification
configuration	ΔE (5 mm) - E (30 cm)
composition	NE110A (or similar)
energy resolution	15%
hardware π^+ ID	μ^+ afterpulse
distance to target	25 cm
$\Delta\Omega$	125 msr
ε_{π^+}	10%

Table 4
A summary of the anticipated π^+ detector parameters.

Appendix A.

2.1.3 Kinematics and count-rate estimate

In Table 5, we summarize our anticipated experimental kinematics:

For a single tagger counter (which subtends 170 keV), we anticipate an experimental π^+ event rate given by

$$\dot{N}_{\pi^+}(E_\gamma,\theta) = \frac{d\sigma}{d\Omega}(E_\gamma,\theta)\cdot\Delta\Omega\cdot t'\cdot\dot{N}_e\cdot\varepsilon_{\rm tagg}\cdot\varepsilon_{\pi^+}, \qquad (1)$$

where $\dot{N}_{\pi^+}$ is the anticipated count rate, $d\sigma/d\Omega$ is the differential cross section [12], $\Delta\Omega$ is the detector solid angle, t' is the areal density of photoproduction centers in the target, $\varepsilon_{\rm tagg}$ is the tagging efficiency, and ε_{π^+} is the π^+ detection efficiency. We summarize these parameters in Table 6.

Our anticipated count rate per tagger counter is thus 2.4 π^+s per hour. We will group the focal plane into 32 bins of two counters each (340 keV per bin). We will accumulate 1080 counts per bin (3% statistics) in 230 hours. The cross section for the C(γ,π^+) background mechanism scales with the atomic number. We thus expect six times the aforementioned π^+ rate from the C component of the CH_2 target. We will remove this contamination from the data with a dedicated run on the matched C target mentioned in Table 3. A 3% statistical measurement per bin of this background will require 40 hours. Sub-threshold spectra will be used in our π^+ random background subtraction.

2.1.4 Beamtime request

Table 7 summarizes our beamtime request for this experiment.

	$\theta_{\pi^+} = 20.0^\circ$		
Eγ (MeV)	T$_{\pi^+}$ (MeV)	T$_n$ (MeV)	θ_n ($^\circ$)
171.0	25.5	4.6	18.9
170.5	25.0	4.6	18.6
170.0	24.5	4.7	18.3
179.5	23.9	4.7	18.0
179.0	23.4	4.7	17.7
178.5	22.9	4.8	17.5
178.0	22.3	4.8	17.2
177.5	21.8	4.8	16.9
177.0	21.3	4.9	16.6
176.5	20.7	4.9	16.3
166.0	20.2	5.0	16.0
165.5	19.6	5.0	15.6
165.0	19.1	5.1	15.3
164.5	18.5	5.1	15.0
164.0	18.0	5.2	14.7
163.5	17.4	5.2	14.4
163.0	16.9	5.3	14.1
162.5	16.3	5.3	13.7
162.0	15.8	5.4	13.4
161.5	15.2	5.4	13.1
161.0	14.6	5.5	12.7
160.5	14.1	5.6	12.4
160.0	13.5	5.7	12.0

Table 5
A summary of our proposed π^+ kinematics. Photons with energy less than 161 MeV create π^+s which probably do not have sufficient kinetic energy to be detected.

As shown, 325 hours of beam on target is sufficient to make a 3% statistical measurement for both the $CH_2(\gamma, \pi^+)$ and $C(\gamma, \pi^+)$ reactions. Given experiment setup time, debugging, and overhead, this experiment will fit nicely into a 3-week time slot.

quantity	value
$< d\sigma/d\Omega >$	5 μb/sr
$\Delta\Omega$	125 msr
t' (CH_2)	300 mg/cm^2 (1.291 $\times$ 10^{22} cm^{-2} C; 2.582 $\times$ 10^{22} cm^{-2} H)
$\dot{N}_e$	1 MHz
$\varepsilon_{\rm tagg}$	40%
ε_{π^+}	10%

Table 6
A summary of the anticipated experiment parameters folded into our π^+ rate estimate for a single tagger counter.

quantity	time (hr)
$CH_2(\gamma,\pi^+)$	230
$C(\gamma,\pi^+)$	40
tagging efficiency	50
background & calibration data	5
total	325

Table 7
An overview of our beam-time request for this experiment.

2.1.5 Summary

With this experiment, we will reproduce the world's data set with a photon energy resolution of 340 keV and a 3% statistical error over the energy regime roughly 9-20 MeV above threshold using moderate resolution plastic telescopes. Detecting the μ^+ afterpulses associated with the decay of the π^+s will provide an unambiguous means of particle identification complementary to standard ΔE-E techniques. The two-body final state from the p(γ,π^+)n reaction will provide precise π^+ energy calibration for the detector telescopes. Background measurements performed on a matched C wafer will facilitate background subtractions. The (γ,p) and (γ,d) reactions will be measured simultaneously. A standard, well-understood tagged-photon data analysis is anticipated [11,13,14].

Because of its self-calibrating and self-normalizing nature, we feel this experiment is an excellent candidate with which to initiate the π^+ photoproduction program at the upgraded MAX-lab tagged photon facility.

2.2 π^+ photoproduction via coincident detection of the π^+ and the neutron very close to threshold

2.2.1 Overview

In this second experiment in the anticipated program, we shall measure absolute cross sections for $\gamma + p \longrightarrow n + \pi^+$ very close to the reaction threshold (E_γ = 151.44 MeV) using the high-resolution tagged photon facility at MAX-lab. Recoil neutrons will be detected in a liquid scintillator array. As in the first experiment (see Section 2.1), π^+s will be detected in well-understood fast plastic ΔE-E scintillator telescopes. We will again employ thin, solid targets to minimize π^+ energy loss and simplify the overall normalization. Particle identification in the neutron array will be performed with pulse-shape discrimination techniques, and neutron energies will be determined using time-of-flight. Our goal is to reproduce the existing world data set using recoil neutrons with a photon energy resolution of 340 keV and a 1% statistical error over the energy regime 2-13 MeV above threshold using the neutron array, and to cross check these results with complementary measurements in the plastic telescopes with an energy resolution of 340 keV to a statistical uncertainty of 2% in the energy regime 9-13 MeV above threshold.

This experiment is constructed as a necessary systematic bridge between the π^+ measurement proposed in Section 2.1, and the high-luminosity recoil neutron measurement proposed in Section 2.3.

2.2.2 Measurement details

Fig. 2 shows an overview of the experiment hall.

Photon beam

We anticipate electron and photon beam characteristics nearly identical to those required for our first measurement (see Section 2.1.2), save for the tagged photon-energy range. For this experiment, we will move the focal-plane arrays to tag an 11 MeV photon-energy bite from 153 MeV $< E_\gamma <$ 164 MeV (corresponding to π^+s from 4.5 MeV $< T_{\pi^+} <$ 18.0 MeV at $\theta_{\pi^+} = 20°$, and neutrons from 7.0 MeV $< T_n <$ 5.2 MeV at $\theta_n = 1°$). Again, we anticipate that π^+s with $T_{\pi^+} <$ 15 MeV will be energetically forbidden from reaching the detectors, so that the effective π^+ tagging range will be 160 MeV $< E_\gamma <$ 164 MeV. However, this overlap region is, as it provides us with a cross check on the absolute normalization of the neutron measurements.

Targets and detectors (X-arm)

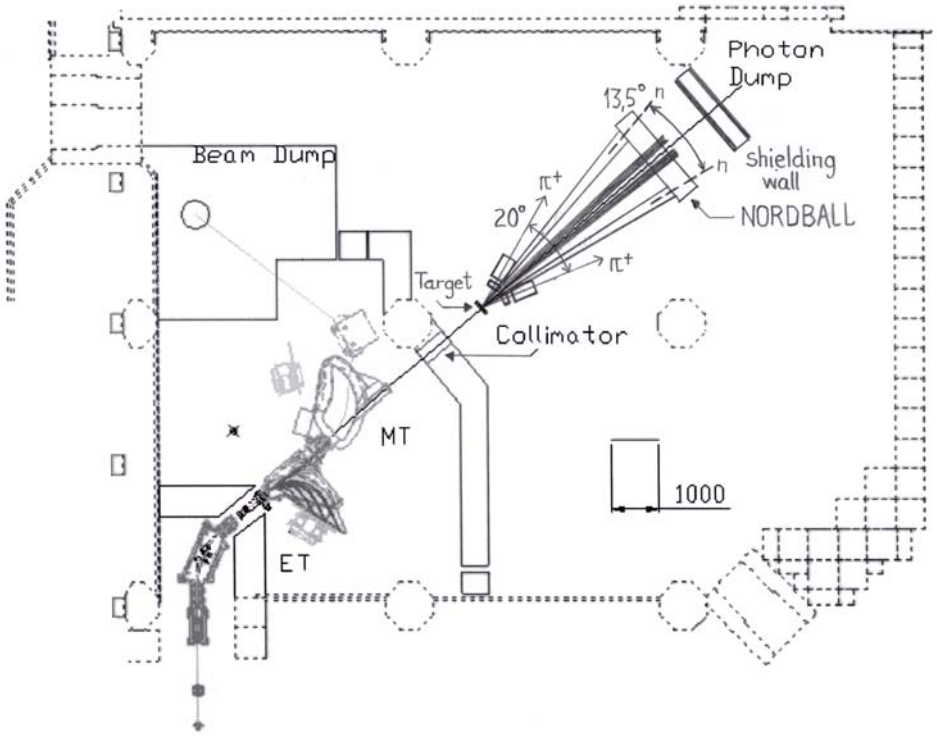

Fig. 2. The proposed configuration of the experiment hall for this experiment. The π^+ telescope configuration is identical to that proposed in Section 2.1.

Quantity	Description
E_{beam}	200 MeV
I_{beam}	10 nA
radiator	100 μm Al
tagger	SAL end-point (ET)
focal-plane array	Lund 64-counter(40 counters below π^+ threshold)
E_γ bite	153 MeV $< E_\gamma <$ 164 MeV (11 MeV)
ΔE_γ	170 keV
$\dot{N}_e$ per counter	1 MHz
collimator	12 mm diameter
absolute $\varepsilon_{\rm tagg}$ measurements	multiple
relative $\varepsilon_{\rm tagg}$ measurements	yes
$\varepsilon_{\rm tagg}$	40%

Table 8
A summary of the anticipated beam parameters. These parameters have been established based on experience gained at SAL [5] and MAX-lab [6].

Target	Thickness (mg/cm^2)
CH_2	300
C	255
blank	N/A

Table 9
A summary of the anticipated target parameters. The thickness of CH_2 is chosen as a trade-off between event rate and π^+ energyloss in the target. The thickness of C is chosen to match the C-content of the CH_2 target.

Quantity	Specification
configuration	ΔE (5 mm) - E (30 cm)
composition	NE110A (or similar)
energy resolution	15%
hardware π^+ ID	μ^+ afterpulse
distance to target	25 cm
$\Delta\Omega$	125 msr
$\varepsilon_{\pi+}$	10%

Table 10
A summary of the anticipated π^+ detector parameters.

For this measurement, we will again use the thin solid targets described in the previous experiment (see Section 2.1.2).

We will employ ΔE-E plastic scintillator telescopes identical in all aspects to those used for the first measurement as π^+ detectors (see Section 2.1.2).

We will also employ the NORDBALL detector (see Appendix B.2 for a complete description) to search for recoil neutrons. The NORDBALL detector consists of a series of pentagonal (6) and hexagonal (10) cells containing organic liquid scintillator. The MeV$_{ee}$ energy calibration of the detector (which essentially determines the neutron detection efficiency ε_n), will be obtained using a PuBe source [15]. Particle identification (discrimination between photons and neutrons) is performed via pulse-shape discrimination (PSD) [16]. A thin plastic scintillator veto may be used to reject charged particles. Neutron kinetic energy will be determined using time-of-flight techniques (see [17]). The neutron detection efficiency will be simulated using such codes as STANTON [18]. The simulated values for ε_n will be cross-checked against dedicated efficiency measurements using the techniques based upon ^{252}Cf fragmentation presented in [19] and recently expanded upon in [20,21]. And ultimately, because of the two-body final state, ε_n will be unambiguously determined over the region of acceptance overlap with the π^+ telescopes (since the absolute

Quantity	Specification
configuration	(veto) - NORDBALL cell
composition	liquid organic scintillator
energy resolution	4%
hardware π^+ ID	pulse-shape discrimination
distance to target	5 m
geometeric $\Delta\Omega$	hexagonal - 0.9 msr; pentagonal - 0.6 msr
ε_n	25%

Table 11
A summary of the anticipated neutron detector parameters.

detection efficiency of these devices is well known).

Within a few MeV of reaction threshold, neutrons recoil in a rather small cone which is forward peaked and symmetric about the photon beam in the laboratory. We will configure the 10 hexagonal elements (each with an 8.4 cm effective radius) of the NORDBALL array in an annulus about the photon beam at a distance of 5 m from the targets, a distance sufficient for an energy resolution of 4% [22]. Each element will be positioned so that a neutron with a laboratory angle of 1° will be incident upon the center of the cell. Neutron kinetic energies T_n will vary between 4-7 MeV. We anticipate a detection threshold of 1.5 MeV_{ee}, corresponding to ε_n of about 25%. This will leave an aperature with a diameter of 9 cm for the photon beam to pass through. Neutrons which correspond to the π^+s we detect in the ΔE-E scintillator telescopes have average $T_n = 5.3$ MeV and angles $13.1° < \theta_n < 14.7°$. We will position two of the pentagonal NORDBALL elements (each with a 7.0 cm effective radius) on either side of the photon beam in the horizontal plane, one at 13.5° and one at 14.5°. The final two pentagonal elements will be placed at 7.3° on either side of the beam, to bridge the gap between the two primary configurations.

2.2.3 Kinematics and count-rate estimate

In Tables 12, 13 and 14, we summarize our anticipated experimental kinematics:

For a single tagger counter which subtends 170 keV in the energy range 161.5 MeV $< E_\gamma <$ 164 MeV, we anticipate an experimental π^+ event rate given by

$$\dot{N}_{\pi^+}(E_\gamma,\theta) = \frac{d\sigma}{d\Omega}(E_\gamma,\theta)\cdot\Delta\Omega\cdot t'\cdot\dot{N}_e\cdot\varepsilon_{\rm tagg}\cdot\varepsilon_{\pi^+}, \qquad (2)$$

Eγ (MeV)	θ_{π^+} (°)	T_{π^+} (MeV)	T_n (MeV)	θ_n (°)
164.0	20.0	18.0	5.2	14.7
163.7	20.0	17.6	5.2	14.5
163.5	20.0	17.4	5.2	14.4
163.0	20.0	16.9	5.3	14.1
162.5	20.0	16.3	5.3	13.7
162.2	20.0	15.9	5.4	13.5
162.0	20.0	15.8	5.4	13.4
161.5	20.0	15.2	5.4	13.1
161.0	20.0	14.6	5.5	12.7
160.5	20.0	14.1	5.6	12.4
160.0	20.0	13.5	5.7	12.0

Table 12
A summary of our proposed π^+ kinematics. Photons with energy less than 161.5 MeV create π^+s which probably do not have sufficient kinetic energy to be detected. NORDBALL cells will be placed at $\theta_n = 13.5$ ° and 14.5°, so that the both the π^+s and the recoil neutrons will be detected in coincidence.

where $\dot{N}_{\pi^+}$ is the anticipated count rate, $d\sigma/d\Omega$ is the differential cross section [12], $\Delta\Omega$ is the detector solid angle, t' is the areal density of photoproduction centers in the target, $\varepsilon_{\rm tagg}$ is the tagging efficiency, and ε_{π^+} is the π^+ detection efficiency.

Furthermore, for an identical tagger counter at any location along the focal plane of the tagging spectrometer, we expect an experimental recoil neutron rate given by

$$\dot{N}_n(E_\gamma,\theta) = \frac{d\sigma}{d\Omega}(E_\gamma,\theta)\cdot\Delta\Omega\cdot t'\cdot\dot{N}_e\cdot\varepsilon_{\rm tagg}\cdot\varepsilon_n\cdot\varepsilon_{\rm live}, \qquad (3)$$

where $\dot{N}_n$ is the anticipated count rate, ε_n is the neutron detection efficiency, $\varepsilon_{\rm live}$ is the electronics livetime, and all other variables have been defined previously. We include and electronics livetime term in Eqn. 3 since the π^+ telescopes are capable of dramatically different rates than the neutron cells. We summarize these parameters in Table 15.

Our anticipated neutron count rate per tagger counter is 15 neutrons per hour. For the recoil neutron analysis, we will group the focal plane into 32 bins of four counters each (340 keV per bin). We will accumulate 10000 counts per

	$\theta_n = 7.3°$			$\theta_n = 13.5°$			$\theta_n = 14.5°$		
Eγ (MeV)	$\theta_{\pi+}$ (°)	$T_{\pi+}$ (MeV)	T_n (MeV)	$\theta_{\pi+}$ (°)	$T_{\pi+}$ (MeV)	T_n (MeV)	$\theta_{\pi+}$ (°)	$T_{\pi+}$ (MeV)	T_n (MeV)
164.0	8.9	18.7	4.4	17.9	18.2	5.0	19.6	18.0	5.1
163.5	9.1	18.2	4.5	18.4	17.6	5.1	20.3	17.4	5.2
163.0	9.4	17.6	4.5	19.0	17.0	5.2	20.9	16.8	5.3
162.5	9.6	17.0	4.6	19.6	16.4	5.3	21.6	16.2	5.5
162.0	9.9	16.4	4.7	20.2	15.7	5.4	22.6	15.5	5.6
161.5	10.2	15.8	4.8	20.9	15.1	5.5	22.3	14.9	5.7
161.0	10.5	15.3	4.9	21.7	14.5	5.7	23.2	14.2	5.9
160.5	10.8	14.7	5.0	22.6	13.8	5.8	24.1	13.6	6.1
160.0	11.2	14.1	5.1	23.5	13.2	6.0	25.1	12.9	6.2
159.5	11.6	13.4	5.2	24.6	12.5	6.1	26.3	12.2	6.4
159.0	12.0	12.8	5.3	25.8	11.8	6.3	27.6	11.5	6.7
158.5	12.4	12.2	5.4	27.2	11.1	6.6	29.1	10.7	6.9
158.0	13.0	11.6	5.6	28.9	10.3	6.8	31.0	9.9	7.3
157.5	13.5	10.9	5.7	31.0	9.5	7.1	33.4	8.9	7.7
157.0	14.2	10.3	5.8	33.8	8.6	7.5	36.6	7.6	8.5
156.5	14.9	9.6	6.0	38.0	7.6	8.0	-	-	-
156.0	15.7	8.9	6.2	-	-	-	-	-	-
155.5	16.7	8.2	6.4	-	-	-	-	-	-
155.0	17.8	7.5	6.6	-	-	-	-	-	-
154.5	19.3	6.7	6.9	-	-	-	-	-	-
154.0	21.2	5.9	7.2	-	-	-	-	-	-
153.5	23.9	5.0	7.6	-	-	-	-	-	-
153.0	29.0	3.8	8.3	-	-	-	-	-	-

Table 13

A summary of our proposed bridge kinematics for the NORDBALL elements placed in the plane of the laboratory at $\theta_n = 7.3°$, 13.5°, and 14.5°. Photons with energy less than 161.5 MeV create π^+s which probably do not have sufficient kinetic energy to be detected in the π^+ detector(s) at $\theta_{\pi+} = 20°$. The NORDBALL cells placed on either side of the photon beam at $\theta_n = 13.5°$, and 14.5° will detect recoil neutrons in coincidence with π^+s. The NORDBALL cells placed on either side of the photon beam at $\theta_n = 7.3°$ detect neutrons which lie in the gap between the two primary configurations.

	$\theta_n = 1.0^\circ$		
Eγ (MeV)	θ_{π^+} ($^\circ$)	T$_{\pi^+}$ (MeV)	T$_n$ (MeV)
164.0	1.2	18.9	4.2
163.5	1.2	18.4	4.3
163.0	1.2	17.8	4.3
162.5	1.3	17.2	4.4
162.0	1.3	16.7	4.5
161.5	1.3	16.1	4.6
161.0	1.4	15.5	4.6
160.5	1.4	14.9	4.7
160.0	1.5	14.3	4.8
159.5	1.5	13.7	4.9
159.0	1.6	13.1	5.0
158.5	1.6	12.5	5.1
158.0	1.7	11.9	5.2
157.5	1.8	11.3	5.3
157.0	1.8	10.7	5.5
156.5	1.9	10.4	5.6
156.0	2.0	9.4	5.7
155.5	2.1	8.7	5.9
155.0	2.2	8.1	6.1
154.5	2.4	7.4	6.3
154.0	2.5	6.7	6.5
153.5	2.7	5.9	6.7
153.0	3.0	5.1	7.0

Table 14

A summary of our proposed dedicated neutron kinematics for the NORDBALL elements forming an annulus at $\theta_n = 1.0^\circ$ about the beam direction. Photons with energy less than 161.5 MeV create π^+s which probably do not have sufficient kinetic energy to be detected in the π^+ detector(s) at $\theta_{\pi^+} = 20^\circ$.

quantity	value
$< d\sigma/d\Omega >_{\pi^+}$	5 μb/sr
$< d\sigma/d\Omega >_{\rm neutron}$	4 μb/sr
$\Delta\Omega_{\pi^+}$	125 msr
$\Delta\Omega_{\rm neutron}$	600 msr (annulus element)
t' (CH_2)	300 mg/cm^2 (1.291×10^{22} cm^{-2} C; 2.582×10^{22} cm^{-2} H)
$\dot{N}_e$	1 MHz
$\varepsilon_{\rm tagg}$	40%
$\varepsilon_{\rm live}$	50%
ε_{π^+}	10%
ε_n	25%

Table 15
A summary of the anticipated experiment parameters folded into our neutron rate estimate for a single tagger counter.

bin (1% statistics) bin in 335 hours in each element of the annulus. We will use PSD photon spectra for our neutron random background subtraction. We will measure the C background with a dedicated run on the C target (see below).

Our anticipated π^+ count rate per tagger counter is identical to that obtained for the first measurement in the series - 2.4 π^+s per hour per counter (see Section 2.1.3). For the π^+ analysis, we will group the focal plane into 32 bins of four counters each. The 335-hour counting time defined by the neutron measurement will result in 1600 π^+s per bin. Since the configuration is identical to that used in the first measurement, we will be able to combine the statistics of the two measurements in a straightforward fashion, thereby improving our overall statistical uncertainty to 2.5% for the overlap region. We will again measure the C background to 3% statistics per bin with a dedicated 40-hour run. Sub-threshold spectra will be used in our π^+ random background subtraction.

2.2.4 Beamtime request

Table 16 summarizes our beamtime request for this experiment.

As shown, 450 hours of beam on target is sufficient to make a 1% statistical measurement of the recoil neutron, and simultaneously increase our statistics for the π^+ channel (within the overlap region) to 2%. Given experiment setup time, debugging, and overhead, this experiment will fit into a 3-week time slot.

quantity	time (hr)
$CH_2(\gamma, \pi^+)$ and $CH_2(\gamma, n)$	335
$C(\gamma, \pi^+)$ and $C(\gamma, n)$	40
tagging efficiency	50
background & calibration data	25
total	450

Table 16
An overview of our beam-time request for this experiment.

2.2.5 Summary

With this experiment, we will measure recoil neutrons with a photon energy resolution of 340 keV and a 1% statistical error over the energy regime roughly 2-13 MeV above threshold using the NORDBALL neutron array. We will simultaneously cross check these results with complementary measurements using plastic scintillator telescopes to a statistical uncertainty of 2% in the energy regime 9-13 MeV above threshold using the techniques outlined in the first experiment (see Section 2.1). A standard, well-understood tagged-photon data analysis is again anticipated [2,11,13,14].

This experiment is constructed as a necessary systematic bridge between the π^+ measurement proposed in Section 2.1, and the high-luminosity recoil neutron measurement proposed in Section 2.3.

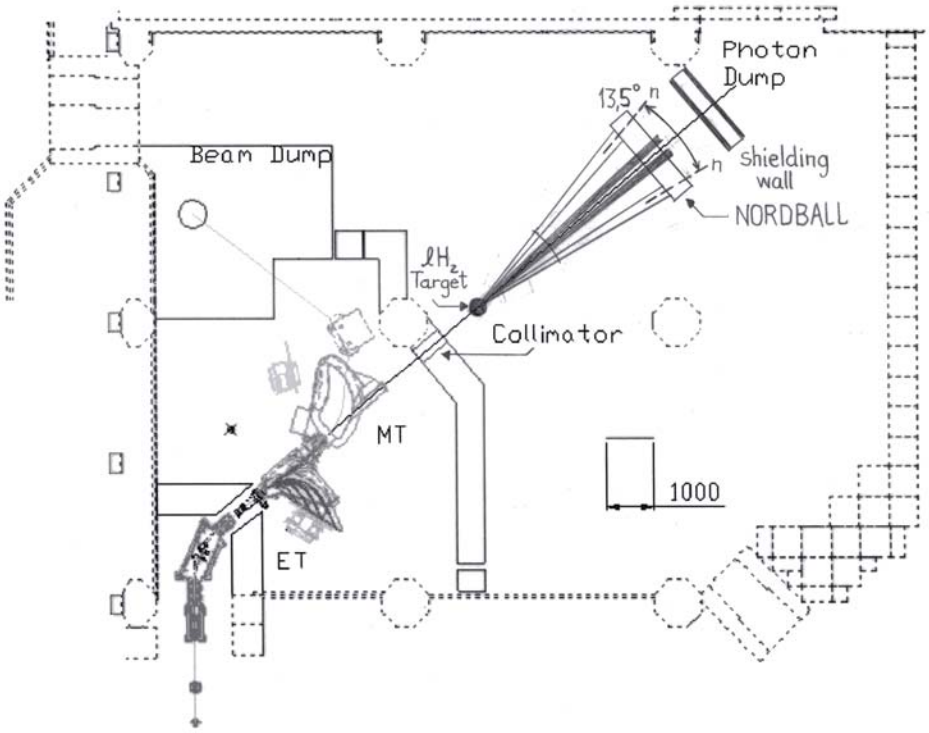

Fig. 3. The proposed configuration of the experiment hall for this experiment The NORBALL configuration is identical to that proposed in Section 2.2.

2.3 High-luminosity measurements of threshold π^+ photoproduction

2.3.1 Overview

In this third experiment in the anticipated program, we shall measure absolute cross sections for $\gamma + p \longrightarrow n + \pi^+$ across the reaction threshold ($E_\gamma = 151.44$ MeV) using the high-resolution tagged photon facility at MAX-lab. Recoil neutrons will be detected in a liquid scintillator array configured identically to that employed in the previous experiment (see Section 2.2). We will utilize an overhauled and slightly modified version of the Lund ℓD_2 target (which we will now refer to as the Lund ℓH_2 target). Our goal is to reproduce world results with a photon energy resolution of 170 keV and a 3% statistical error over the energy regime 0-12 MeV above threshold using the neutron array.

This measurement will improve on the best photon-energy resolution so-far achieved in this type of measurement by about a factor of two [2]. Statistical precision will be on the level of 1%.

2.3.2 Measurement details

Fig. 3 shows an overview of the experiment hall.

Quantity	Description
E_{beam}	200 MeV
I_{beam}	10 nA
radiator	100 μm Al
tagger	SAL end-point (ET)
focal-plane array	Lund 64-counter(40 counters below π^+ threshold)
E_γ bite	150 MeV $< E_\gamma <$ 161 MeV (11 MeV)
ΔE_γ	170 keV
$\dot{N}_e$ per counter	1 MHz
collimator	12 mm diameter
absolute $\varepsilon_{\rm tagg}$ measurements	multiple
relative $\varepsilon_{\rm tagg}$ measurements	yes
$\varepsilon_{\rm tagg}$	40%

Table 17
A summary of the anticipated beam parameters. These parameters have been established based on experience gained at SAL [5] and MAX-lab [6].

Photon beam

We anticipate electron and photon beam characteristics nearly identical to those required for our second measurement (see Section 2.3.2), save for the tagged photon-energy range. For this experiment, we will move the focal-plane arrays to tag an 11 MeV photon-energy bite from 150 MeV (sub-threshold) $< E_\gamma <$ 161 MeV (corresponding to neutrons from 8.9 MeV $< T_n <$ 4.6 MeV at $\theta_n = 1^\circ$). Our sub-threshold measurement is again useful for the purposes of calibrations and background subtractions.

Targets and detectors (X-arm)

For this measurement, we will use the Lund ℓH_2 target (see Appendix C for a complete description). After consultations with local ([23,24]) and international ([25]) cryogenic target experts, we are confident that a minor maintenance overhaul and some slight modifications to the existing target will enable us to safely liquify hydrogen. The target cell is 16.4 cm long, and the density of ℓH_2 is 0.07 gm/cm^3.

We will again employ the NORDBALL detector (see Appendix B.2 for a complete description) in a configuration identical to that proposed in the second experiment (see Section 2.2.2) to search for recoil neutrons. The identical configuration is very important, as the understanding of the previous neutron

Target	Thickness (g/cm^2)
ℓH_2	1.148
empty	N/A

Table 18
A summary of the anticipated target parameters.

Quantity	Specification
configuration	(veto) - NORDBALL cell
composition	liquid organic scintillator
energy resolution	4%
hardware π^+ ID	pulse-shape discrimination
distance to target	5 m
geometric $\Delta\Omega$	hexagonal - 0.9 msr; pentagonal - 0.6 msr
ε_n	25%

Table 19
A summary of the anticipated neutron detector parameters. These parameters are identical to those proposed for the second experiment (see Table 11).

measurement normalization (see Section 2.2) will be directly applicable to this measurement, providing a good cross check of our final results.

2.3.3 Kinematics and count-rate estimate

In Table 20, we summarize our anticipated experimental kinematics:

For a single tagger counter which subtends 170 keV in the energy range 151 MeV $< E_\gamma <$ 161 MeV, we anticipate an experimental recoil neutron event rate given by

$$\dot{N}_n(E_\gamma,\theta) = \frac{d\sigma}{d\Omega}(E_\gamma,\theta)\cdot\Delta\Omega\cdot t'\cdot\dot{N}_e\cdot\varepsilon_{\rm tagg}\cdot\varepsilon_n\cdot\varepsilon_{\rm live}, \qquad (4)$$

where $\dot{N}_n$ is the anticipated count rate, $d\sigma/d\Omega$ is the differential cross section [12], $\Delta\Omega$ is the detector solid angle, t' is the areal density of photoproduction centers in the target, $\varepsilon_{\rm tagg}$ is the tagging efficiency, ε_n is the neutron detection efficiency, and $\varepsilon_{\rm live}$ is the electronics livetime. We anticipate a free-running focal plane for this experiment.

We summarize these parameters in Table 21.

Our anticipated count rate per tagger counter is thus 235 neutrons per hour.

	$\theta_n = 1.0^\circ$		
Eγ (MeV)	θ_{π^+} ($^\circ$)	T$_{\pi^+}$ (MeV)	T$_n$ (MeV)
161.0	1.4	15.5	4.6
160.5	1.4	14.9	4.7
160.0	1.5	14.3	4.8
159.5	1.5	13.7	4.9
159.0	1.6	13.1	5.0
158.5	1.6	12.5	5.1
158.0	1.7	11.9	5.2
157.5	1.8	11.3	5.3
157.0	1.8	10.7	5.5
156.5	1.9	10.4	5.6
156.0	2.0	9.4	5.7
155.5	2.1	8.7	5.9
155.0	2.2	8.1	6.1
154.5	2.4	7.4	6.3
154.0	2.5	6.7	6.5
153.5	2.7	5.9	6.7
153.0	3.0	5.1	7.0
152.5	3.4	4.3	7.4
152.0	4.0	3.3	7.8
151.5	5.8	1.8	8.9
151.0	-	-	-
150.5	-	-	-
150.0	-	-	-

Table 20
A summary of our proposed dedicated neutron kinematics for the NORDBALL elements forming an annulus at $\theta_n = 1.0^\circ$ about the beam direction.

We will accumulate 10000 counts per counter (1% statistics) in 50 hours. We will use both (random) background photons as well as events corresponding to our sub-threshold tagger counters in our background subtraction.

quantity	value
$< d\sigma/d\Omega >_{\rm neutron}$	3 μb/sr
$\Delta\Omega_{\rm neutron}$	600 msr (annulus element)
t' (H)	1.148 g/cm^2 (6.914×10^{23} cm^{-2})
$\dot{N}_e$	1 MHz
$\varepsilon_{\rm tagg}$	40%
$\varepsilon_{\rm live}$	50%
ε_n	25%

Table 21
A summary of the anticipated experiment parameters folded into our neutron rate estimate for a single tagger counter.

quantity	time (hr)
production target running	50
tagging efficiency	50
background & calibration data	25
total	125

Table 22
An overview of our beam-time request for this experiment.

2.3.4 Beamtime request

Table 22 summarizes our beamtime request for this experiment.

As shown, 125 hours of beam on target is sufficient to make a 1% statistical measurement. Given experiment setup time, debugging, and overhead (especially target overhead), this experiment will fit nicely into a 3-week time slot.

2.3.5 Summary

In this experiment, we will use the NORDBALL neutron array and the Lund ℓH_2 target to make a high-luminosity measurement of π^+ photoproduction over the energy regime roughly 0-10 MeV above threshold. A standard, well-understood, tagged-photon data analysis is again anticipated [2,11,13,14].

This measurement will improve on the best photon-energy resolution so-far achieved in this type of measurement by about a factor of two [2]. Statistical precision will be on the level of 1%.

2.4 Threshold Photoproduction of π^+

2.4.1 Overview

In the fourth measurement in the anticipated program, we will use the high-resolution tagged photon facility at MAX-lab together with an active scintillator target to measure the absolute cross sections for the $\gamma + p \longrightarrow n + \pi^+$ reaction very close to the reaction threshold, $E_\gamma = 151.44$ MeV.

We will detect the emitted π^+s in the scintillating target, and recoil neutrons will also be detected using the NORDBALL liquid scintillator array. This array will be configured identically to the previous measurement (see Section 2.3), which will serve as a cross check on the active scintillator results.

The goal is to generate cross sections less than 0.5 MeV from the pion photoproduction threshold with a photon energy resolution of 170 keV and better than 2% statistical uncertainty over the energy range up to a few MeV above reaction threshold.

This measurement will improve upon the best previous measurement of this fundamental process in terms of photon energy resolution, statistics, and proximity to reaction threshold.

2.4.2 Measurement Details

Close to threshold, the pion has very little kinetic energy and cannot exit any target of reasonable thickness. The most recent measurement of this reaction [2] avoided this problem by detecting the recoil neutron (emitted in a cone centered about the photon beam direction) in a liquid scintillator detector array. The maximum angle of the neutron increases with photon energy, and below about 1 MeV from threshold, the neutron angle is too close to the photon beam to permit detection of the neutron. Thus, in order to get even closer to threshold, the π^+ must be detected. We propose to do this by using an active scintillator target together with pulse-shape discrimination (PSD) techniques to identify and eliminate background due to other photoreactions in the target scintillator material.

Pion production from the proton will produce a minimum-ionizing pion with a well-defined energy. Other photoreactions will produce knock-on protons of much higher energies, and these will have a different energy-loss signature in the scintillator. Due to the properties of liquid scintillator, the shape of the light output pulse is different depending on the ionization produced by the charged particle, allowing us to separate minimum ionizing pions from heavier particles. Another source of background will be Compton scattering of the

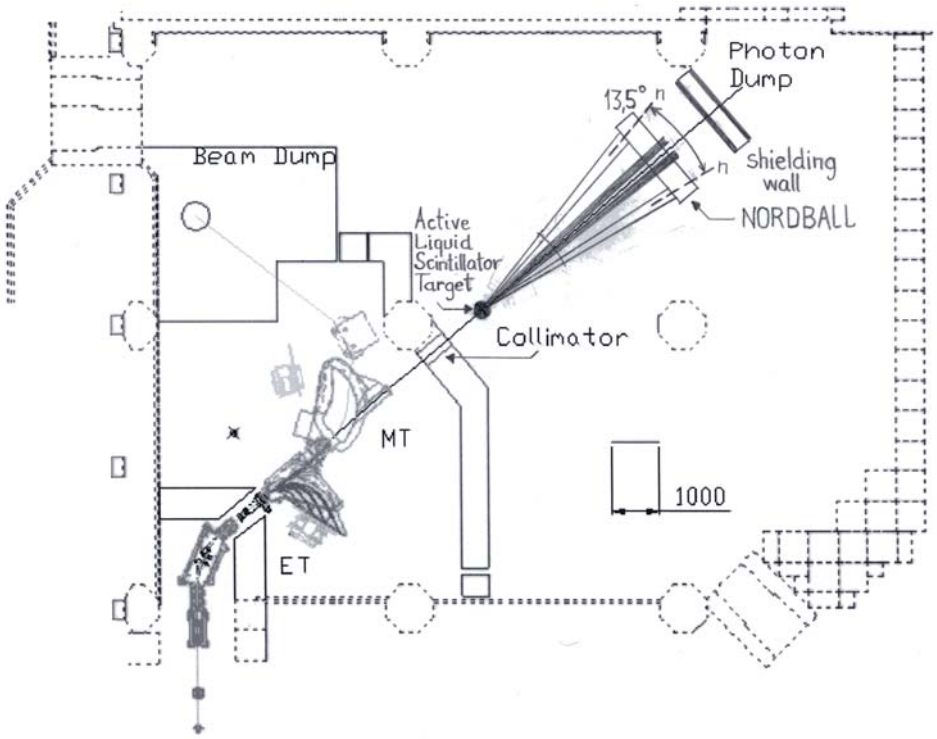

Fig. 4. The proposed configuration of the experiment hall for this experiment The NORBALL configuration is identical to that proposed in Section 2.3.

beam photons. Here, the knock-on electron is also a minimum-ionizing particle; however, its energy will typically be quite different from the energy of the pions, and this can be used to distinguish events from this background source. Finally, the 4.12 MeV μ^+ produced in the decay of the π^+ ($\tau_{\rm mean} = 26.0$ ns) should provide an additional method for identification of the π^+ events. The portion of the focal plane configured below pion photoproduction threshold will provide a measure of background-only events which we can use to test and confirm our understanding of the background for photon energies above threshold.

Particle identification will be performed both at the hardware and software levels via well-established techniques. Our goal is to produce absolute cross sections with a photon energy resolution of about 170 keV and a 2% statistical error over the energy regime from threshold to a few MeV above threshold. The higher energy data can be compared with the results determined by detecting the recoil neutron, both in this measurement and in earlier measurements, using a ℓH_2 target performed as a part of the planned experimental program, as well as with the existing data on this channel. We anticipate this will provide a stringent test of both our π^+ event identification and the final background subtraction.

Fig. 4 shows an overview of the experiment hall.

Photon beam

We anticipate using a machine setup similar to the previous experiment (see Section 2.3.2), with the only change being a reduced beam current to reduce the count rate in the active target to give acceptable levels of pile-up. We will thus use a low-current 200 MeV CW electron beam, incident on a thin bremsstrahlung radiator (50 μm Al). The duty-factor of the beam will be continuously monitored throughout the data taking [4]. We will employ the (former) SAL end-point tagger (ET) [5] together with the Lund focal-plane array (64 counters) [6] to tag photons with energies from 150 MeV to 161 MeV with a per-counter resolution of approximately 170 keV [8]. The above combination of electron beam and tagger parameters should produce a recoil electron rate per tagger counter of about 10 kHz. We anticipate collimating the photon beam to 12 mm in diameter to ensure its incidence upon the target volume while providing an acceptable tagging efficiency value, anticipated to be approximately 40% with the listed parameters.

Multiple, dedicated low-intensity tagging efficiency measurements will be performed throughout the production data-taking period in order to determine the absolute photon flux incident on the target. Continual monitoring of the *relative* tagging efficiency will be performed during the production running, using a dedicated stand-alone beam monitor [7].

Approximately one quarter of the focal-plane counters will be tagging photons with energies below the pion photoproduction threshold. Data in coincidence with these sub-threshold tagger channels will be used measure background-only events which will be used to test and confirm our understanding of the background for the photon energies above threshold.

2.4.3 Target and detectors (X-arm)

Pions produced close to threshold will be detected in an active liquid scintillator target. Pulse-shape discrimination techniques, based on the difference in light output produced by charged particles with different ionization densities as they traverse the scintillator material, will be used to discriminate between π^+ events and events produced by other photoreactions in the target. We will also use a π^+ identification method based on the 4.12 MeV μ^+ afterpulses associated π^+ decay as a complement to the proposed PSD methods, looking for these decay pulses in a 100 ns window subsequent to the primary π^+ event (as discussed in Section 2.1). As before (see Section 2.1), high-quality delay lines with low dispersion and low loss (RG-8 or better) will be used to optimize the quality of the detector signals.

A hardware coincidence between the recoil electron in the tagger focal plane and the X-arm will be made. The maximum beam current will be determined

Quantity	Description
E_{beam}	200 MeV
I_{beam}	1 nA
radiator	50 μm Al
tagger	SAL end-point (ET)
focal-plane array	Lund 64-counter (20 counters below π^+ threshold)
E_γ bite	150 MeV $< E_\gamma <$ 161 MeV (11 MeV)
ΔE_γ	170 keV
$\dot{N}_e$ per counter	10 kHz
collimator	12 mm diameter
absolute ε_{tagg} measurements	multiple
relative ε_{tagg} measurements	yes
ε_{tagg}	40%

Table 23
A summary of the anticipated beam parameters.These parameters have been established based on experience gained at SAL [5] and MAX-lab [6].

by the level of pile-up in the active target.

The NORDBALL neutron detector array will be configured identically to the previous experiment in the planned program, see Section 2.3.2. The identical configuration is very important, as the understanding of the previous neutron measurement normalization (see Section 2.3) will be directly applicable to this measurement, providing a good cross check of our final results.

2.4.4 Kinematics and count-rate estimates

The desired NORDBALL kinematics are presented in Table 20.

Liquid scintillator has a H density of 6.27×10^{22} atoms/cm^3. Assuming a 2.5 cm long target and (since the π^+s are detected within the target) a nearly 4π acceptance and 100% detection efficiency, an estimate of the count rate can be made. Some pions produced near the ends of the target may not be contained within the target volume, reducing the final acceptance. The details of the acceptance will be addressed using a GEANT Monte-Carlo simulation.

For a single tagger counter (which subtends 170 keV), we anticipate a π^+ event

quantity	value
$< d\sigma/d\Omega >$	3 μb/sr
$\Delta\Omega$	$\sim 4\pi$ sr
t' (H)	1.57×10^{23} cm^{-2}
$\dot{N}_e$	10 kHz
$\varepsilon_{\rm tagg}$	40%
ε_{π^+}	$\sim$ 100%
$\varepsilon_{\rm live}$	50%

Table 24
A summary of the anticipated experiment parameters folded into our π^+ rate estimate for a single tagger counter.

rate given by,

$$\dot{N}_{\pi^+}(E_\gamma,\theta) = \frac{d\sigma}{d\Omega}(E_\gamma,\theta)\cdot\Delta\Omega\cdot t'\cdot\dot{N}_e\cdot\varepsilon_{\rm tagg}\cdot\varepsilon_{\pi^+}\cdot\varepsilon_{\rm live} \qquad (5)$$

where $\dot{N}_{\pi^+}$ is the anticipated count rate, $d\sigma/d\Omega$ is the differential cross section [12], $\Delta\Omega$ is the detector solid angle, t' is the areal density of photoproduction centers in the target, $\varepsilon_{\rm tagg}$ is the tagging efficiency, ε_{π^+} is the π^+ detection efficiency, and $\varepsilon_{\rm live}$ is the electronics livetime.

These parameters are summarized in Table 24.

Our anticipated π^+ count rate per tagger counter is thus about 30 events per hour. We will accumulate about 4000 events (which corresponds to a 2% statistical uncertainty) in 130 hours. This should provide a final uncertainty, after background subtraction, of about 3% in the π^+ cross sections. Reducing this final statistical uncertainty to 2% would require about 260 hours of beam on target.

2.4.5 Beamtime request

Table 7 summarizes our beamtime request for this experiment.

We estimate that 335 hours of beam time should be sufficient to make a measurement of the $\gamma + p \longrightarrow \pi^+ + n$ cross section very close to threshold with a final statistical uncertainty of 2%. Given experiment setup time, debugging, and overhead, this experiment will fit nicely into a 3-week time slot.

quantity	time (hr)
production target running	260
tagging efficiency	50
background & calibration data	25
Total	335

Table 25
An overview of our beam-time request.

2.4.6 Summary

With this experiment, we will measure the $\gamma + p \longrightarrow \pi^+ + n$ cross section in the first 5 MeV above threshold with a photon energy resolution of about 170 keV and a 2% statistical uncertainty.

This measurement will improve upon the best previous measurement of this fundamental process in terms of photon energy resolution, statistics, and proximity to reaction threshold.

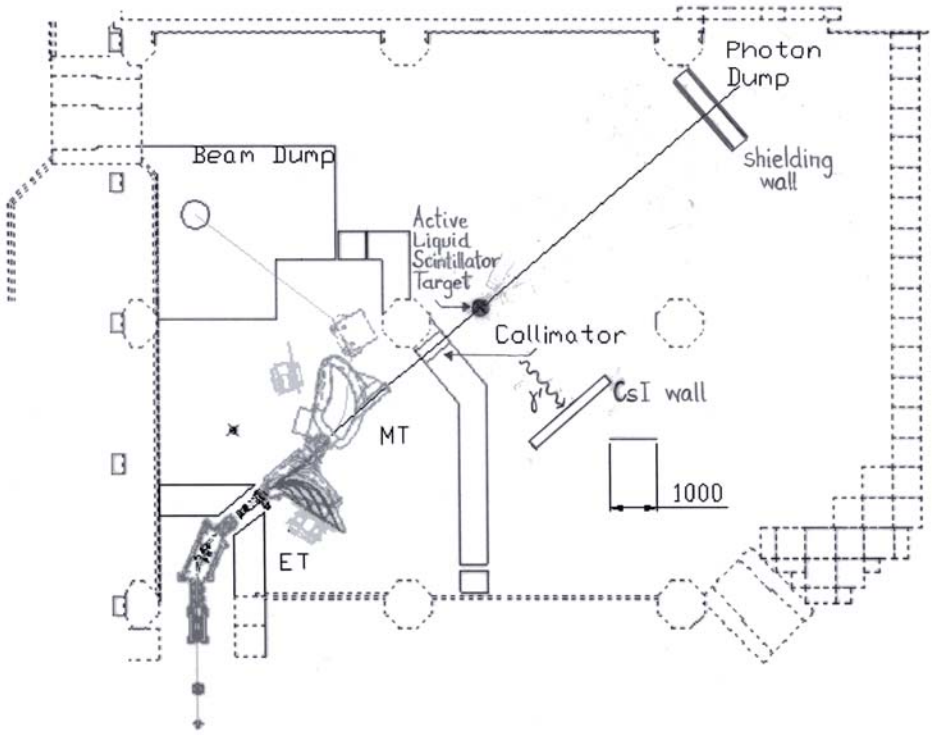

Fig. 5. The proposed configuration of the experiment hall for this experiment.

2.5 Near-threshold Photoproduction of π^-

2.5.1 Overview

In this measurement, we intend to build on the experience obtained in the previous measurement with an active scintillator target, and use a now-deuterated scintillator to measure the absolute cross sections for the $\gamma + n \longrightarrow p + \pi^-$ reaction close to the reaction threshold, $E_\gamma = 151.44$ MeV. Such a measurement of the photoproduction channel will provide new, important information on the $E_{0+}^{(\pi^- p)}$ amplitude, and form a useful test of the existing π^- capture measurement $\pi^- + p \longrightarrow n + \gamma$ performed at TRIUMF[3]. It would also provide an independent measure of the E_{0+} amplitude for the $\pi^- p$ channel.

This measurement will match or improve upon the best previous measurement of this fundamental process, provide a cross check against a recent measurement of the inverse reaction, and greatly expand the available data set.

2.5.2 Measurement details

Fig. 5 shows an overview of the experiment hall.

Near threshold, the pion is produced with a very little kinetic energy. It will thus be stopped within the target volume, where it will be captured. An energetic gamma-ray together with a recoil particle will result. We propose to detect this 129 MeV photon from the π^- capture using a large volume CsI detector in coincidence with a scintillation event in the active target to identify $\gamma + n \longrightarrow p + \pi^-$ events.

The monoenergetic photon resulting from the π^- capture provides a very clean signal to identify the events of interest. The largest source of background will come from Compton scattering of beam photons from the target nuclei; however, by judicious choice of CsI detector angle and the range of tagged photon energies we can ensure these background events can be identified and reliably subtracted. In addition, the portion of the data obtained at photon energies below the pion photoproduction threshold will provide a measure of background-only events which we can use to test and confirm our understanding of the background for photon energies above threshold.

The CsI gamma-ray detector efficiency and response function will be determined by simulation together with direct measurement of the detector line shape by placing the detector in the tagged photon beam (at a significantly reduced intensity). These measurements will also provide an energy calibration of the detector system. Additional effort will be required to model (in a GEANT Monte-Carlo simulation) the target system to ensure we fully understand the acceptance and background contributions.

Photon beam

We anticipate using a machine setup similar to the previous experiment which measured $p+\gamma \longrightarrow n+\pi^+$ using an active scintillator target (see Section 2.4). We will use a low-current 200 MeV CW electron beam, incident on a thin bremsstrahlung radiator (50 μm Al). The duty-factor of the beam will be continuously monitored throughout the data taking [4]. We will employ the (former) SAL end-point tagger (ET) [5] together with the Lund focal-plane array (64 counters) [6] to tag photons with energies from 150 MeV to 161 MeV with a per-counter resolution of approximately 170 keV [8]. The above combination of electron beam and tagger parameters should produce a recoil electron rate per tagger counter of about 10 kHz. We anticipate collimating the photon beam to 12 mm in diameter to ensure its incidence upon the target volume, while providing an acceptable tagging efficiency value, anticipated to be approximately 40% with the listed parameters.

Multiple, dedicated low-intensity tagging efficiency measurements will be performed throughout the data taking period in order to determine the absolute photon flux incident on the target. Continual monitoring of the *relative* tagging efficiency will be performed during the production running using a dedicated

Quantity	Description
E_{beam}	200 MeV
I_{beam}	1 nA
radiator	50 μm Al
tagger	SAL end-point (ET)
focal-plane array	Lund 64-counter (20 counters below π^+ threshold)
E_γ bite	150 MeV $< E_\gamma <$ 161 MeV (11 MeV)
ΔE_γ	170 keV
$\dot{N}_e$ per counter	10 kHz
collimator	12 mm diameter
absolute ε_{tagg} measurements	multiple
relative ε_{tagg} measurements	yes
ε_{tagg}	40%

Table 26
A summary of the anticipated beam parameters.These parameters have been established based on experience gained at SAL [5] and MAX-lab [6].

stand-alone beam monitor [7].

Approximately one quarter of the focal-plane counters will be tagging photons with energies below the pion photoproduction threshold. Data in coincidence with these sub-threshold tagger channels will be used measure background-only events which will be used to test and confirm our understanding of the background for the photon energies above threshold.

2.5.3 Target and detectors (X-arm)

Pions produced close to threshold will be detected in an active liquid scintillator target, and the 129 MeV capture photon will be detected in a large volume CsI detector [2] Pulse-shape discrimination techniques, based on the difference in light output produced by charged particles with different ionization densities, will be used to discriminate between π^- events and events produced by other photoreactions in the target.

A hardware coincidence between the recoil electron in the tagger focal plane and the X-arm will be made. The maximum beam current will be determined

[2] according to Bent Schröder, the local photonuclear group is examining the feasiblity of assembling a lattice of CsI(Tl) or CsI(Na) scintillators to detect photons above 60 MeV. We will use this lattice.

by the level of pile-up in the active target.

2.5.4 Kinematics and count-rate estimates

Liquid scintillator has a deuterium density of 4.06×10^{22} atoms/cm^3. We anticipate the 2.5 cm long target proposed for the earlier active target measurement, resulting in a D density of 1.02×10^{23} atoms/cm^2. Since the π^- will convert within the target, the acceptance will be defined by the gamma-ray detector acceptance and detection efficiency. Assuming a 10 cm collimation for the CsI detector located 1 meter from the target, the acceptance will be 30 msr. Some pions produced near the ends of the target may not be contained within the target volume and thus lost, reducing the final acceptance. The details of the acceptance will be addressed using a GEANT Monte-Carlo simulation.

For a single tagger counter (which subtends 170 keV), we anticipate a π^- event rate given by,

$$\dot{N}_{\pi^-}(E_\gamma, \theta) = \frac{d\sigma}{d\Omega}(E_\gamma, \theta) \cdot \Delta\Omega \cdot t' \cdot \dot{N}_e \cdot \varepsilon_{\rm tagg} \cdot \varepsilon_{\pi^-} \cdot \varepsilon_{\rm live} \qquad (6)$$

where $\dot{N}_{\pi^-}$ is the anticipated count rate, $d\sigma/d\Omega$ is the differential cross section [12], $\Delta\Omega$ is the detector solid angle, t' is the areal density of photoproduction centers in the target, $\varepsilon_{\rm tagg}$ is the tagging efficiency, ε_{π^+} is the π^- detection efficiency, and $\varepsilon_{\rm live}$ is the electronics livetime.

These parameters are summarized in Table 27.

quantity	value
$< d\sigma/d\Omega >$	3 μb/sr
$\Delta\Omega$	30 msr
t' (D)	1.02×10^{23} cm^{-2}
$\dot{N}_e$	10 kHz
$\varepsilon_{\rm tagg}$	40%
ε_{π^-}	$\sim$100%
$\varepsilon_{\rm live}$	$\sim$100%

Table 27
A summary of the anticipated experiment parameters folded into our π^- rate estimate for a single tagger counter.

Our anticipated π^- count rate per tagger counter is thus about 2 events per

hour. We will accumulate about 1000 events (which corresponds to a 3% statistical uncertainty) in 500 hours. Grouping the focal plane into 32 bins of 2 counters each (340 keV per bin), will cut our counting times in half, requiring about 250 hours of beam on target. This should provide a final uncertainty (after background subtraction) of about 4% in the π^- cross sections.

2.5.5 Beamtime request

Table 28 summarizes our beamtime request for this experiment.

quantity	time (hr)
production target running	250
tagging efficiency	50
background & calibration data	25
Total	325

Table 28
An overview of our beam-time request.

We estimate that 325 hours of beam time should be sufficient to make a measurement of the $\gamma + n \longrightarrow \pi^- + p$ cross section very close to threshold with a final statistical uncertainty of about 4%. Given experiment setup time, debugging, and overhead, this experiment will fit nicely into a 3-week time slot.

2.5.6 Summary

With this experiment, we will measure the $\gamma + n \longrightarrow \pi^- + p$ cross section in the first 5 MeV above threshold with a photon energy resolution of about 340 keV and a 4% statistical uncertainty.

This measurement will match or improve upon the best previous measurement of this fundamental process, provide a cross check against a recent measurement of the inverse reaction, and greatly expand the available data set.

3 Summary

The experiment program is summarized in Table 29.

Name	E_γ (MeV)	ΔE_γ (keV)	δ_{stat} (%)	detected particle	beam time (hr)	real time (week)
Near threshold $H(\gamma,\pi^+)$	161.5 - 171.0	340	3.0	π^+	325	3
π^+ photoproduction via coincident detection of the π^+ and neutron	161.5 - 164.0	(340)	(2.0)	(π^+)		
very close to threshold	153.0 - 164.0	340	1.0	neutron	450	3
High-luminosity measurements of threshold π^+ photoproduction	(150.0) - 161.0	170	3.0	neutron	125	3
Threshold Photoproduction of π^+	(150.0) - 161.0	170	2.0	π^+	335	3
Near-threshold Photoproduction of π^-	(150.0) - 161.0	340	4.0	π^-,γ'	325	3

Table 29
An overview of the proposed series of experiments.

We anticipate that a total of 1560 hours of beamtime (5 three-week blocks) will be necessary to successfully complete this program.

4 Acknowledgements

We wish to acknowledge the invaluable contributions and guidance of W. Briscoe, K. Hansen, M. Hoegerl, M. Lundin, D. Meekins, B. Nilsson, A. Reiter, and I. Strakovsky in the generation of this proposal.

References

[1] V. Bernard, New developments in threshold pion photoproduction and electroproduction, `http://arXiv.org/abs/hep-ph/9710430`, (1997).

[2] E. Korkmaz *et al.*, Measurement of the $\gamma p \to \pi^+ n$ Reaction near Threshold, Phys. Rev. Lett. **83**, 3609 (1999).

[3] M. A. Kovash for the E643 Collaboration, Total cross-sections for π^- p $\to \gamma$ n at 10-MeV to 20-MeV, PiN Newsletter **12N3**, 51 (1997).

[4] J. M. Vogt and R. Florizone, A duty factor monitor for use with a near cw electron beam, Nucl. Instrum. and Meth. **A339**, 425 (1994).

[5] J. M. Vogt *et al.*, The photon tagging facility at the Saskatchewan Accelerator Laboratory, Nucl. Instrum. and Meth. **A324**, 198 (1993).

[6] J. -O. Adler *et al.*, A broad range tagging spectrometer for the MAX-laboratory, Nucl. Instrum. and Meth. **A388**, 17 (1997).

[7] B. Nilsson, Ph. D. thesis, Lund University, in progress.

[8] J. -O. Adler *et al.*, Upgrade of the pulse stretcher and nuclear physics beamline at MAX-lab and the possibilities for a polarised photon beam, Department of Nuclear Physics Photonuclear Group Report 01/01, LUNFD6/(NFFR-3086), 2001.

[9] M. J. Saltmarsh *et al.*, Nucl. Instrum. and Meth. **105**, 311 (1972).

[10] D. Axen *et al.*, Nucl. Instrum. and Meth. **118**, 435 (1974).

[11] K. G. Fissum *et al.*, Inclusive Photoproduction of Positive Pions, Ph. D. thesis, University of Saskatchewan, unpublished (1993).

[12] I. Strakovsky, private communication (2002).

[13] K. G. Fissum *et al.*, Inclusive Positive Pion Photoproduction, Phys. Rev. **C53**, 1278 (1996).

[14] R. O. Owens, Nucl. Instrum. and Meth. **A288**, 574 (1990).

[15] K. J. King, *et al.*, Nucl. Instrum. and Meth. **A227**, 257 (1984).

[16] J. R. M. Annand, A fast module for pulse shape analysis, Nucl. Instrum. and Meth. **A262**, 371 (1987).

[17] J.R.M. Annand, *et al.*, An NE213A TOF spectrometer for high resolution (γ, n) reaction measurements, Nucl. Instrum. and Meth. **A400**, 344 (1997).

[18] R. A. Cecil, *et al.*, Nucl. Instrum. and Meth. **A161**, 439 (1979).

[19] M. Karlsson, Absoulte efficiency calibration of a NE-213 liquid scintillator using a ^{252}Cf source, M. Sc. thesis, Lund University, (unpublished) 1997.

[20] A. Reiter, private communication (2002).

[21] A. Reiter, Ph. D. thesis, University of Glasgow, in progress.

[22] B. -E. Andersson, High Resolution (γ, n) Experiments in Light Nuclei at E_γ = 60 MeV, Ph. D. thesis, Lund University, (unpublished) 1994.

[23] K. Hansen, MAX-lab Cryogenic Target Group, private communication (2002).

[24] M. Lundin, private communication (2002).

[25] D. Meekins and M. Hoegerl, Jefferson Lab Cryogenic Target Group, private communication (2002).

[26] `http://www.bicron.com`

[27] B. -E. Andersson *et al.*, $^{16}O(\gamma, n)$ reaction at intermediate energy Phys. Rev. **C51**, 2553 (1995).

[28] D.A. Sims *et al.*, The (γ, n) study of the isovector quadrupole resonance in ^{40}Ca, alpha-particle wavefunction, Phys. Rev. **C55**, 1288 (1997).

[29] D.A. Sims *et al.*, The $^4He(\gamma, n)$ reaction: a potential testing ground for the alpha-particle wavefunction, Phys. Lett. **B442**, 43 (1998).

[30] I. Akkurt, Ph. D. thesis, University of Glasgow, (unpublished) 1998.

[31] M. Lundin Compton Scattering from the Deuteron at Low Energies, Ph. D. thesis, Lund University, unpublished (2002).

[32] T. Glebe. Diplomarbeit, II. Physikalischen Institut der Georg-August-Universität zu Göttingen, (unpublished) 1993.

[33] W. Briscoe, private communication (2002).

Appendices

A π^+ identification in plastic scintillator telescopes

In this Appendix, we present an overview of the technique behind π^+ identification in fast plastic ΔE-E scintillator telescopes.

The first method of particle identification such a detector affords is via the determination of the charge-to-mass ratio of the incident particle. The thin ΔE-detector acts as a transmission detector, while the thick E-dectector acts as a stopping detector. We will be able to readily distinguish between electrons, pions, protons, and deuterons. Further, by making the analog ESUM of the energy left by the incident particle in the two detectors, we will be able to greatly reduce the number of uninteresting electron events archived (see Fig. A.1).

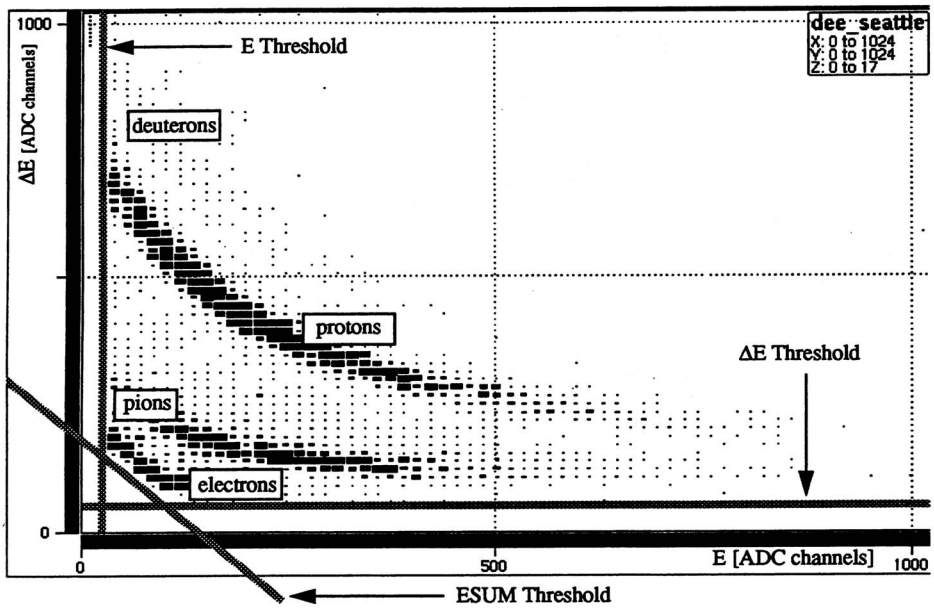

Fig. A.1. The standard ΔE-E technique will allow straightforward separation of electrons, pions, protons, and deuterons. An ESUM threshold will greatly reduce the number of electron events accepted by the electronics.

This method will not help distinguish π^+s from π^-s. For that, we will rely upon the fact that a π^+ will decay to a (μ^+, ν_{μ^+}) pair with a mean lifetime $\overline{\tau}$ = 26.0 ns. Further, the decay μ^+ will have a constant 4.12 MeV kinetic energy. We will thus look for this decay signature using a μADC (which will search for energy subsequent to the primary event pulse consistent with 4.12 MeV), and a μTDC (which will check the decay constant of events labelled as π^+s).

Fig. A.2 shows the energy signature of a typical π^+ event which has stopped and then decayed to a μ^+ in the E-detector.

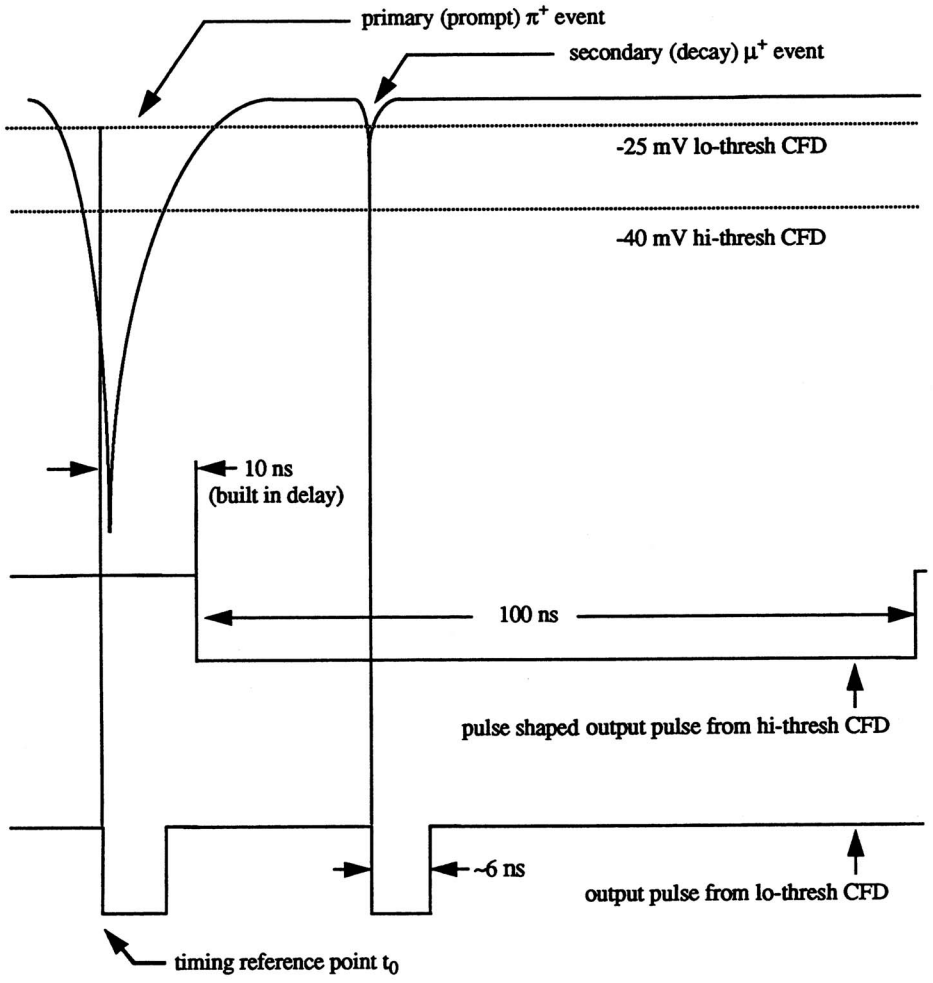

Fig. A.2. Detail of a typical π^+ decay and the characteristics of the discriminators used to identify it.

A pair of discriminators may be used to define a trigger associated with this decay. The first "low-threshold" discriminator will fire on both the prompt π^+ event and the subsequent delay μ^+ event. The second "high-threshold" discriminator will fire only on the prompt π^+ event. By delaying and shaping the "high-threshold" pulse with the circuit shown in Fig. A.3, a μ^+ event trigger may be defined. This event trigger can then be used to stop a μTDC which was started by the focal plane trigger. The resulting spectrum should exhibit the 26 ns mean lifetime of the π^+.

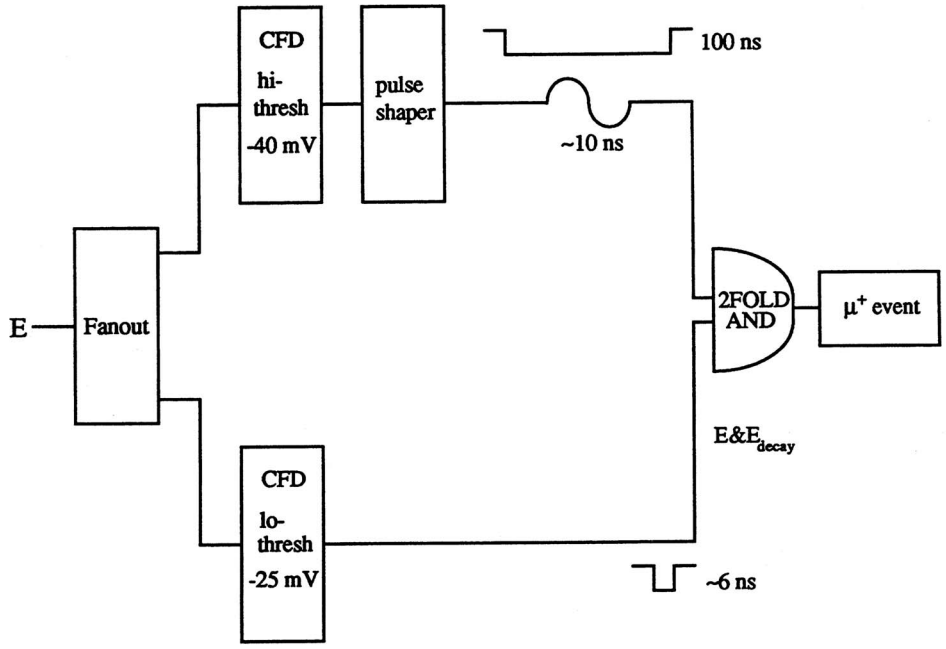

Fig. A.3. A simple circuit which may be used to define a μ^+ event trigger.

The advantage of this method is that the detection efficiency of the circuit itself is easily quantified. Consider Fig. A.4.

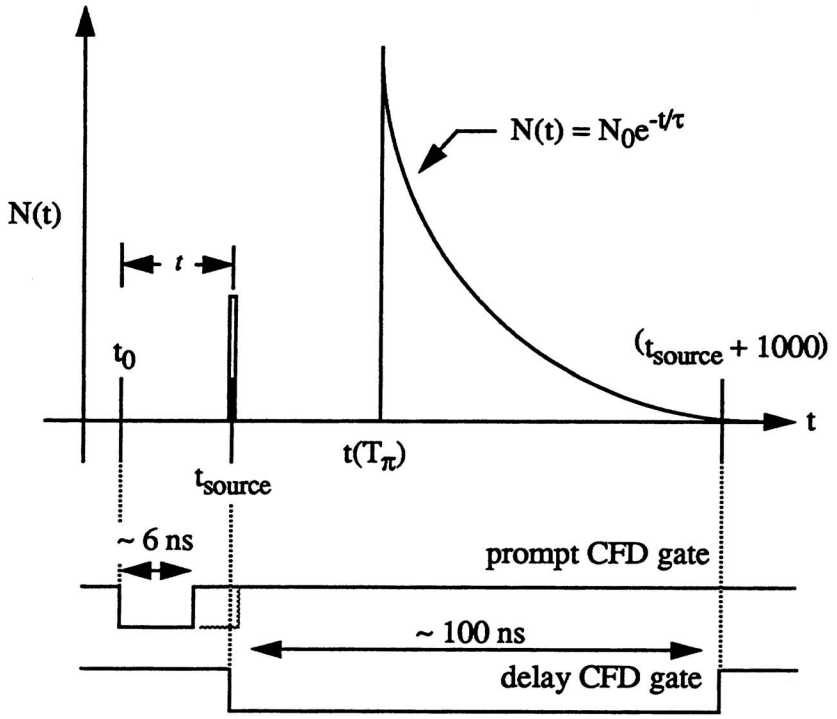

Fig. A.4. The determination of the efficiency of the circuit shown in Fig. A.3.

Here, we have widened the output pulse from the "low-threshold" discriminator so that ALL events (such as those from a source) meet the μ^+ coincidence criterion. This results in a reference spike (t_{source}) in the μTDC spectrum. The gate is then returned to its original (known) width and π^+ data are accumulated. The normalized π^+ detection efficiency is thus given by

$$\varepsilon = \int_{t(T_\pi)}^{t_{source}+100\ ns} dt\ e^{-\frac{t-(t_{source}-6\ ns)}{\overline{\tau}}} \Big/ \int_{t_{source}-6\ ns}^{\infty} dt\ e^{-\frac{t_{source}-6\ ns)}{\overline{\tau}}} \qquad (A.1)$$

where $\overline{\tau}$ is the 26.0 ns mean lifetime of the π^+. $t(T_\pi)$ is simply the edge of the decay distribution in the μTDC spectrum. A typical value for this quantity is 15%.

It is then a simple matter to configure one or more ADCs based on this trigger. A prompt event gate may used to integrate the primary π^+ pulse, while (any number of) delay gates can be used to integrate the μ^+ decay pulse.

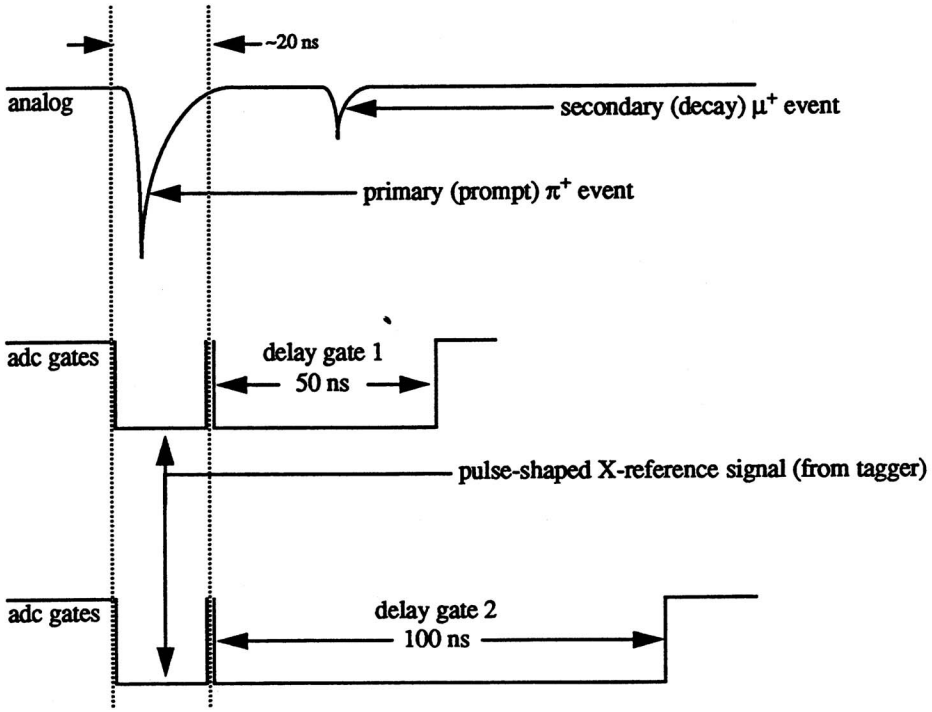

Fig. A.5. Here is a caption.

By plotting the energy deposited in the delay gate against that deposited in the prompt gate (see Fig. A.6), particle identification can be performed.

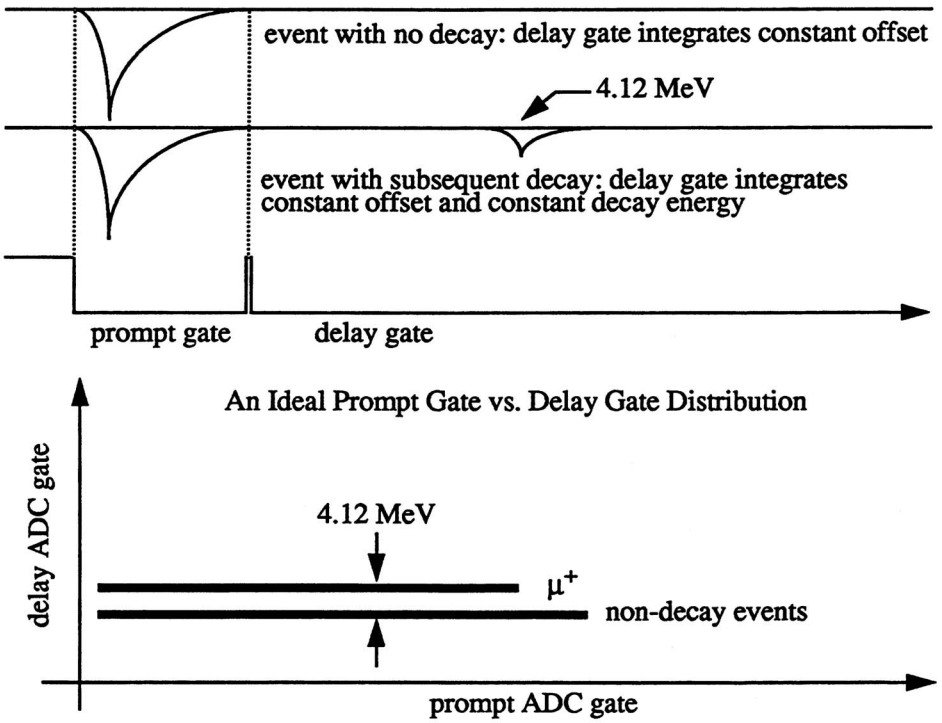

Fig. A.6. Particle identification based on the μADC. In this cartoon figure, we assume monoenergetic π^+s.

This approach works in practice as well as principle, as evidenced in Fig. A.7.

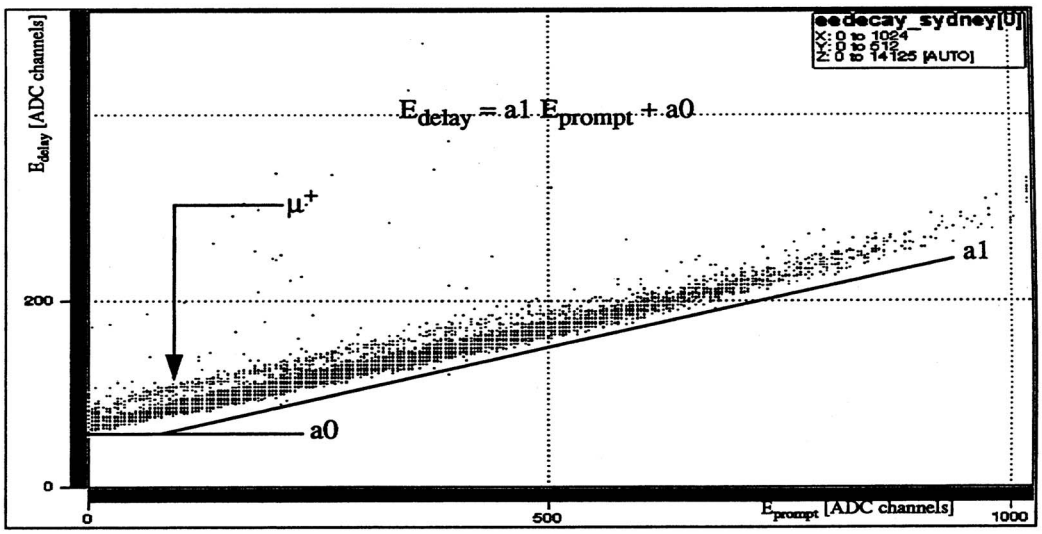

Fig. A.7. Particle identification based on the μADC. The slope of the distribution is due to the varying kinetic energy of the π^+.

B Neutron identification in a liquid scintillator array

In this Appendix, we detail neutron particle identification in organic liquid scintillators, and complement this with a discussion of the NORDBALL detector array.

B.1 Pulse-shape discrimination (PSD)

This section is derived from the thesis work of B. -E. Andersson [22].

The light from most scintillators has a single fast-decay component. However, organic scintillators differ in that they also exhibit a slow-decay component. Differing incident particle types result in differing scintillation decay times. These scintillators can thus be used to perform particle identification based upon the shape of the emitted light pulse. This is known as pulse-shape discrimination (PSD).

The light pulse from the organic scintillator is converted to an anode pulse by the photomultiplier tube. This signal may then be split and passed simultaneously to two charge integrators. As shown in Fig. B.1, one integrates the first 20 ns of the pulse (the fast decay component), while the other integrates the first 500 ns of the pulse (both the fast- and the slow-decay components).

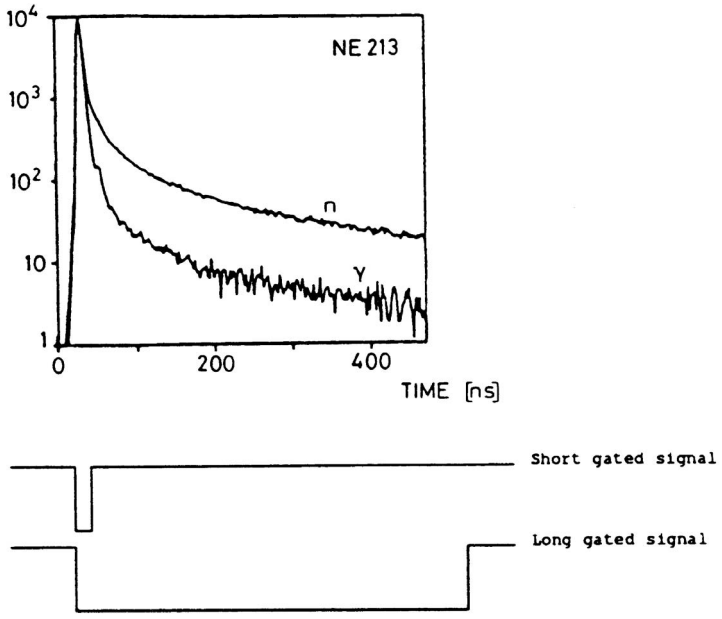

Fig. B.1. The fast and slow components of the scintillation are integrated by gates of dramatically different widths.

The integrated charge is stored in capacitors, and the resulting voltages are passed to both a fast comparator and a analog amplified difference output (PS). The comparator makes a (fast-decay/slow-decay) decision labelling the incident particle type (photons result in fast decays, while neutrons result in slow decays). The amplified difference signal is given by

$$\mathrm{PS} = (\text{long gate}) - \mathrm{ROT} \cdot (\text{short gate}) \tag{B.1}$$

where "long gate" is the long-gated integrated signal, and "short gate" is the short-gated integrated signal, and "ROT" is a scale factor set by a potentiometer and varied to optimize the separation of the fast and slow decay components (see Fig. B.2). A scatterplot of PS vs. LG thus allows for n/γ discrimination over a very large dynamic range via a software cut. It is useful to retain at least some of the γs in the datastream because they constitute a random event distribution useful for background subtractions.

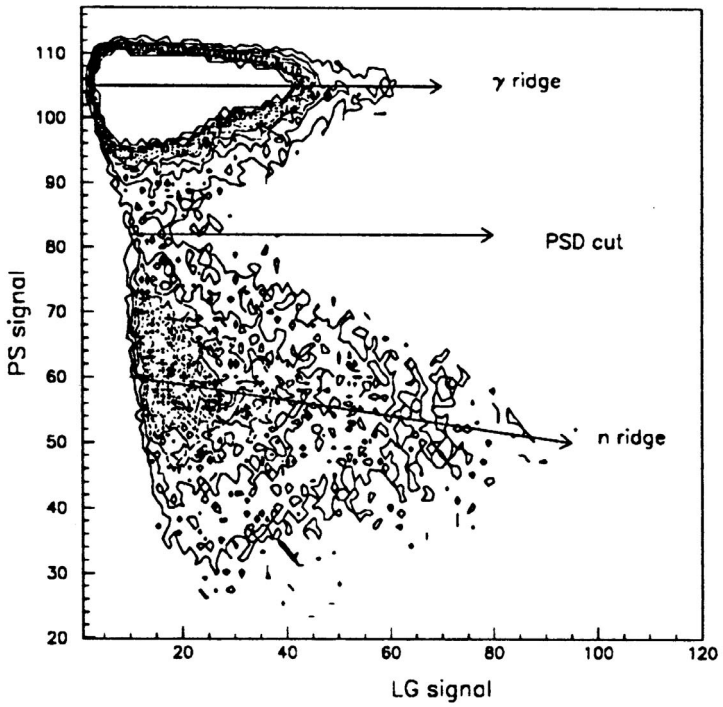

Fig. B.2. A typical PS vs. LG scatterplot showing the excellent separation achieved between γs and neutrons with the PSD method. "ROT" is used to vary the separation between the γ-ridge and the neutron-ridge.

B.2 The NORDBALL detector array

The following description of the NORDBALL apparatus was supplied by A. Reiter [20].

The NORDBALL array [3] consists of 16 (10 hexagonal and 6 pentagonal) elements. The hexagonal elements have a detection radius of 8.4 cm, while the radius of the pentagonal elements is 7.0 cm. Each element consists of a 2 mm stainless steel cell, and is filled with the organic liquid scintillator BC501 [26]. The cells are approximately 15.5 cm deep, so that the active detection volume is 3.33 liters for the hexagonal detectors and 2.57 litres for the smaller pentagons. Each cell is connected to a Philips XP2041, 5-inch diameter PM tube via a 6.35 mm Pyrex glass window (see Figure B.3).

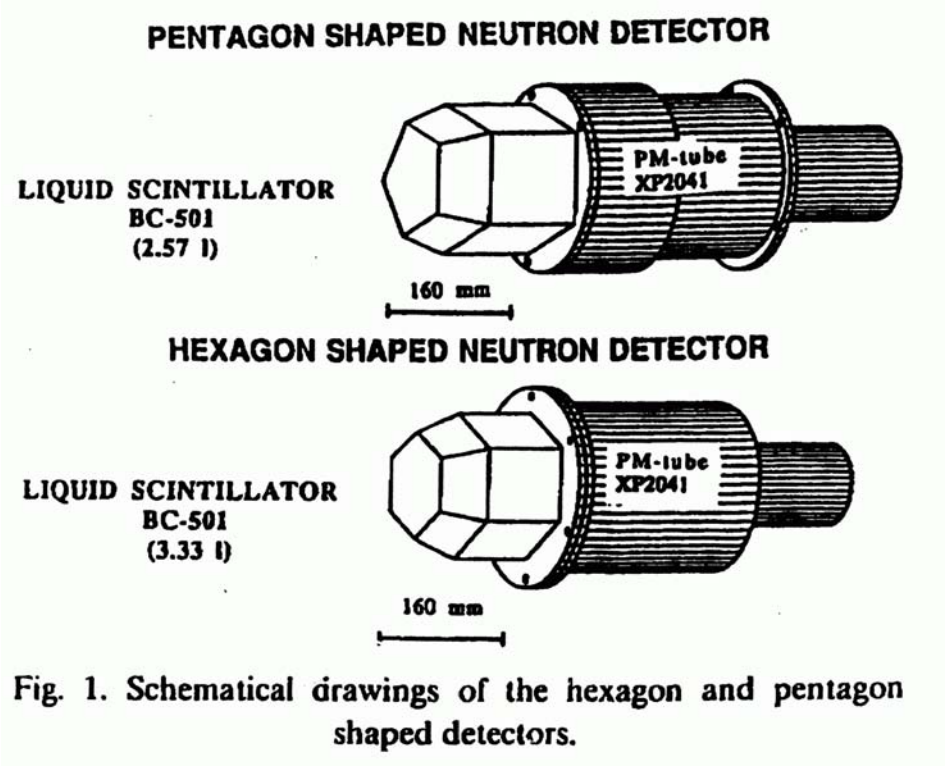

Fig. B.3. A detail of the NORDBALL detector elements.

The current signal is collected from the anode of these tubes. Each detector element may be positioned individually, or mounted onto an purpose-built frame which can allow for the stacking the elements in a predetermined configuration (see Figure B.4).

Organic liquid scintillators offer the possibility of particle identification via pulse-shape discrimination (PSD), a technique which exploits the markedly different dependence of the intensity of the slow component of the scintillation on the type of incident particle. In several previous high-rate, high photon background (γ, n) experiments [2,7,21,27–30], a module developed at the Uni-

[3] currently on loan to the MAX-lab photonuclear group from the University of Göteborg, Sweden.

versity of Glasgow was successfully used to discriminate between photons and neutrons [16]. An overview of a very similar neutron spectrometer is presented in [17].

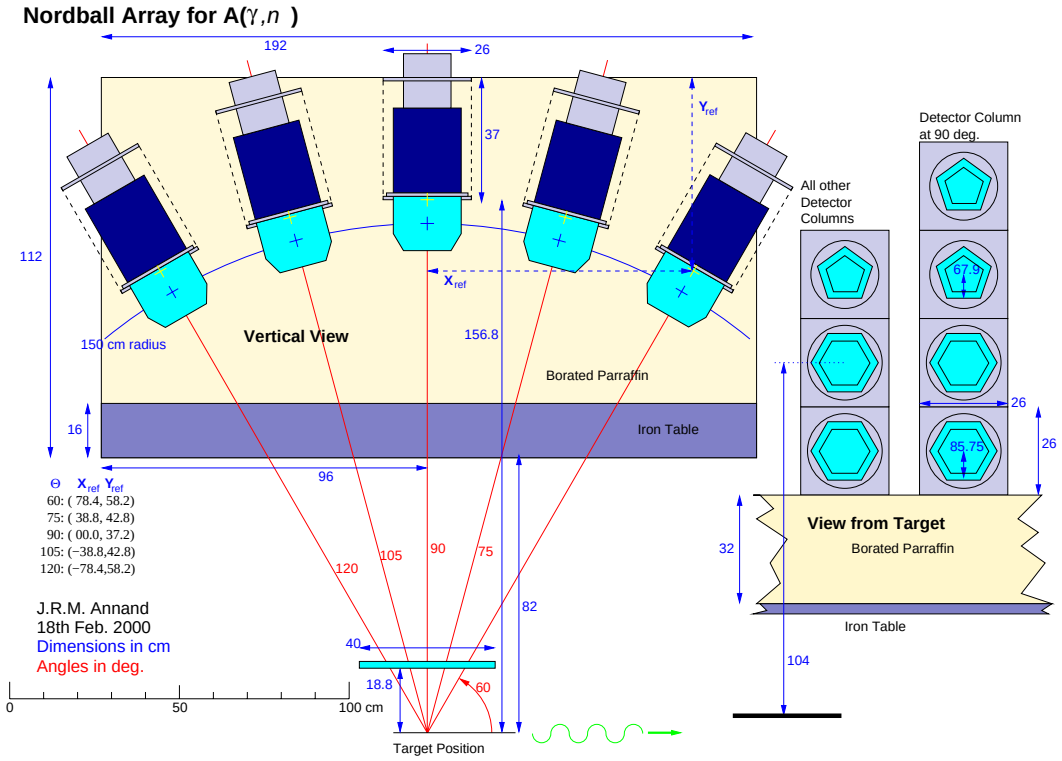

Fig. B.4. An overview of a previously used NORDBALL geometry.

C The Lund ℓD_2 target

The following description of the target was supplied by M. Lundin [31].

The Lund ℓD_2 target was constructed by T. Glebe [32]. The target consists of a target chamber made of 2 mm (1 mm in the scattering plane) stainless steel with 80 mm entrance and 130 mm exit window for the photon beam, as shown in Fig. C.1. The window is a 100 μm Hostaphan foil. A turbo pump creates a vacuum of $\sim 10^{-5}$ mbar [4] in the target chamber. A liquid nitrogen shield inside the chamber reduces the amount of heat radiated onto the interior parts of the target. In thermal connection with the nitrogen shield is a copper plate which shields the cell from the sides and from below.

[4] 1 bar $= 10^5$ Pa.

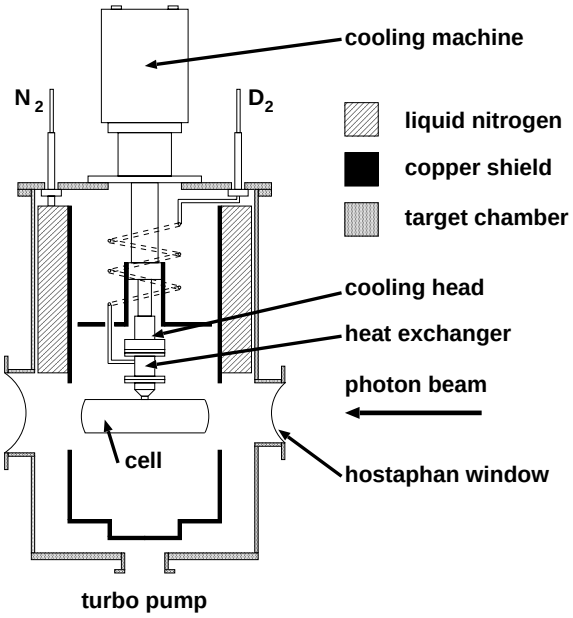

Fig. C.1. A schematic view of the liquid deuterium target.

The cooling machine is mounted on top of the chamber and can reach temperatures as low as 11 K. Since the cooling machine only has two modes (it is either on or off) adjustment of the temperature is done with a small heat element attached to the cooling head of the cooling machine.

The heat exchanger is mounted on the cooling head. Deuterium gas condensates on the heat exchanger and drips down into the cell. The cell is 160 mm in length and 48 mm in diameter and is made of 125 μm Kapton foil. The diameter of the photon beam is typically 35 mm at target position. A two-component adhesive, EPIKOTE and ANCAMIDE, was used during the assembly of the cell. [5]

Two layers of 5 μm super insulation foil are wrapped around the cell to minimize the absorption of thermal radiation. The super insulation foil covering the endcaps has a thin slit to allow a visual check of the liquid deuterium level in the cell.

When the target is run in a steady state, that is, when the amount of liquid deuterium in the cell is constant, the amount of liquid deuterium that boils off

[5] The two component adhesive used to assemble the target cell was EPIKOTE 828 (a trademark of Shell), and ANCAMIDE 260A (a trademark of Air Products and Chemicals Inc). EPIKOTE 828 is a synthetic epoxy resin and ANCAMIDE 260A is the curing agent. The surfaces, Kapton foil or stainless steel, which were to be glued, were polished with steel wool and cleaned with acetone. EPIKOTE and ANCAMIDE were mixed thoroughly for 5 minutes in a weight ratio of 1:1. The adhesive was allowed to set for 2.0 hours at 70°C.

equals the amount of deuterium that condensates on the heat-exchanger and drips down in the cell. The pressure in the system equals the vapor pressure of deuterium for its temperature. Knowledge about the pressure thus makes it possible to determine the temperature of the deuterium liquid. The density of the liquid deuterium is then obtained from the temperature.

The total amount of D_2 is 650 liters at 1150 torr [6] (room temperature) which constitutes a serious safety hazard. Before each experiment, the cell was exposed to a nitrogen pressure of 1500 torr at 80 K. A cell passing this test is expected to withstand 1150 torr at 20 K which is the maximum stress the cell is exposed to while running with deuterium.

The target filling process takes approximately 24 hours, while the emptying process only takes 8 hours. These fairly long periods of time means that no rapid changes between full and empty target measurements can be done.

The target density, ρ, is determined from the pressure of the deuterium gas which was in equilibrium with the deuterium liquid in the cell. Since the pressure varied slightly during a run-period, the pressure was logged for every run (every two hours). The pressure gauge was associated with an error of ± 0.5 torr. For each run-period, the weighted mean pressure, p_{mean}, was determined from the logged pressure p_i and the sum of all focal plane scalers $N_{\gamma,i}$ during that run, for each of the n runs according to

$$p_{mean} = \frac{\Sigma_{i=1}^{n} p_i \, N_{\gamma,i}}{\Sigma_{i=1}^{n} N_{\gamma,i}} \tag{C.1}$$

The target thickness t is given by

$$t = \frac{l_{cell} \ \rho_{mean} \ N_A}{m} \tag{C.2}$$

where l_{cell} is the effective length of the target cell, N_A is Avogadro's number (6.022×10^{23}/mol) and m the molar mass (2.0141 g/mol). The cell length is 0.160 m and the effective cell length is 0.164 ± 0.002 and is due to the convex endcaps of the target cell. Table C.1 shows the target densities and thicknesses for the different run-periods.

[6] 760 torr = 101.325 kPa = 1 atm.

Run-period	$p_{mean}(torr)$	ρ (g/cm^3)	t (10^{23} nuclei /cm^2)
April '96	843 $\pm$ 0.5	0.1622 $\pm$ 0.0005	7.95 $\pm$ 0.14
April '97	772 $\pm$ 0.5	0.1630 $\pm$ 0.0005	7.99 $\pm$ 0.14
September '97	747 $\pm$ 0.5	0.1633 $\pm$ 0.0005	8.01 $\pm$ 0.14

Table C.1
The target densities and thicknesses.

D Liquid scintillator target properties

The following description of the liquid scintillator was supplied by W. Briscoe [33].

D.1 BC-531

D.1.1 General Description

This scintillator provides a combination of properties of particular value to the research physicist. These are:

- Chemical compatibility with nearly all plastics
- High light output
- High flash point
- Moderate cost

BC-531 is particularly suited for intermediate sized detectors in which the containers are fabricated with common plastic materials such as PVC and acrylics. The scintillator provides over twice the light output of mineral oil based liquids having similar plastic compatability.

D.1.2 Properties

Density (at 20 °C)	0.87 g/cm3
Light Output	59% anthracene
Decay Time, Principal Component	3.5 nsec
Wavelength of Maximum Emission	424 nm
Bulk Light Attenuation	3.5 m, minimum
Refractive Index	1.47
Flash Point	93 °C
Atomic Composition:	
No. of H Atoms per cm^3	6.27×10^{22}
No. of C Atoms per cm^3	3.84×10^{22}
Ratio H:C Atoms	1.63
No. of Electrons per cm^3	2.93×10^{23}

D.2 BC-537 — Deuterated Liquid Scintillator

D.2.1 General Description

This liquid scintillator is based on specially purified deuterated benzene. It is particularly useful as a neutron detector and in the study of specific interactions such as n + D. BC-537's appreciable pulse shape discrimination properties also make it useful for neutron-gamma discrimination. BC-537 is encapsulated in Bicron's range of glass and aluminum cells.

In addition to BC-537, Bicron supplies deuterated liquid scintillators having higher D:C ratios or higher D:H ratios.

D.2.2 Properties

Density (at 20 °C)	0.954 g/cm3
Light output	61% anthracene
Wavelength of maximum emission	425 nm
Decay time, principal component	2.8 nsec
Refractive index	1.50
Atomic Composition:	
No. of D Atoms per cm^3	4.06×10^{22}
No. of H Atoms per cm^3	3.55×10^{20}
No. of C Atoms per cm^3	4.10×10^{22}
Ratio D:H Atoms	114
Ratio D:C Atoms	0.99
No. of Electrons per cm^3	2.87×10^{23}